The Use of Scaffold-free Cell Sheet Technique to Refine Mesenchymal Stromal Cell-based Therapy for Heart Failure

Takuya Narita[1], Yasunori Shintani[1], Chiho Ikebe[1], Masahiro Kaneko[1], Niall G Campbell[1], Steven R Coppen[1], Rakesh Uppal[1], Yoshiki Sawa[2], Kenta Yashiro[1] and Ken Suzuki[1]

[1]*William Harvey Research Institute, Barts and The London School of Medicine and Dentistry, Queen Mary University of London, London, UK;* [2]*Department of Cardiovascular Surgery, Osaka University Graduate School of Medicine, Osaka, Japan*

Transplantation of bone marrow-derived mesenchymal stromal cells (MSCs) is an emerging treatment for heart failure based on their secretion-mediated "paracrine effects". Feasibility of the scaffoldless cell sheet technique to enhance the outcome of cell transplantation has been reported using other cell types, though the mechanism underpinning the enhancement remains uncertain. We here investigated the role of this innovative technique to amplify the effects of MSC transplantation with a focus on the underlying factors. After coronary artery ligation in rats, syngeneic MSCs were grafted by either epicardial placement of MSC sheets generated using temperature-responsive dishes or intramyocardial (IM) injection. Markedly increased initial retention boosted the presence of donor MSCs persistently after MSC sheet placement although the donor survival was not improved. Most of the MSCs grafted by the cell sheet technique remained resided on the epicardial surface, but the epicardium quickly regressed and new vessels sprouted into the sheets, assuring the permeation of paracrine mediators from MSCs into the host myocardium. In fact, there was augmented upregulation of various paracrine effect-related genes and signaling pathways in the early phase after MSC sheet therapy. Correspondingly, more extensive paracrine effects and resultant cardiac function recovery were achieved by MSC sheet therapy. Further development of this approach towards clinical application is encouraged.

Received 9 September 2012; accepted 27 December 2012; advance online publication 29 January 2013. doi:10.1038/mt.2013.9

INTRODUCTION

Recent research has shown that transplantation of bone marrow-derived mesenchymal stromal cells (MSCs) is a promising new approach for the treatment of heart failure.[1–4] Although differentiation of MSCs to cardiomyocytes does not occur to a significant extent *in vivo*,[3,4] the ability of MSCs to secrete beneficial growth factors, cytokines, and chemokines is thought to be substantial enough to achieve therapeutic effects by restoring damaged cardiac tissues (known as the paracrine effect).[1,2,5] There is also evidence that MSCs stimulate endogenous progenitor/stem cells towards myocardial regeneration in a paracrine manner.[6,7] Based on these findings, many clinical trials of MSC transplantation are ongoing.[8]

Intramyocardial (IM), intracoronary, or intravenous injection of MSC suspensions is currently used for MSC delivery in the trials, however, these may be suboptimal in achieving the maximum effect from MSC-based therapy. Most importantly, these methods result in poor retention and impeded survival of donor cells, leading to poor donor cell engraftment and consequently to limited therapeutic effects.[2,9–11] Usually, enzymatic digestion (*i.e.*, trypsinization) is used for harvesting MSCs from culture dishes, but this may cause damage to the cells.[12,13] In addition, IM injection causes mechanical damage and inflammation, which will also hinder donor cell survival.[9–11] On the other hand, intracoronary injection of MSCs, having a relatively large cell size, has a risk of coronary embolism,[14] particularly when injected into diseased and narrowed coronary arteries.

Okano and his colleagues have recently developed a novel bioengineering technology to generate scaffold-free "cell sheets" using unique culture dishes, the surface of which is coated with a temperature-responsive polymer (poly-N-isopropylacrylamide).[12,13] At 37 °C the dish surface is hydrophobic, and cells can adhere and grow. However, when the temperature is dropped to 25 °C, the polymer becomes hydrophilic and swollen, causing the cells to detach from the dish as a free cell sheet. In contrast to trypsinization, cell surface proteins, cell–cell junctions, and the underpinning extracellular matrix are well preserved in this method.[12,13] As all polymer remains on the culture dishes throughout the process for cell sheet generation, the produced cell sheets are free of artificial scaffolds.

It has been reported that epicardial placement of cell sheets formed using various cell types improved cardiac function of the damaged heart.[13,15–18] However, even though bone marrow-derived MSCs are one of the most promising donors for cell therapy, the efficiency of cell sheets formed of this cell type has not been reported. Although adipose tissue-derived MSCs have been previously examined,[15,17] the fundamental biological features of these cell types, such as differentiation, viability, proliferation, and stress response, are considerably different.[19] Furthermore, whereas the augmented therapeutic effects by the cell sheet technique have been suggested when compared with other cell delivery methods,[16,20] the

Correspondence: *Ken Suzuki, William Harvey Research Institute, Barts and The London School of Medicine and Dentistry, Charterhouse Square, London, EC1M 6BQ, UK. E-mail: ken.suzuki@qmul.ac.uk*

Table 1 Cardiac function at day 28 after treatment

	HR (bpm)	LVEF (%)	LVDd (mm)	LVDs (mm)	AWTd (mm)	PWTd (mm)	MV E/A
Echocardiography							
Control	418.8 ± 11.6	36.1 ± 1.4	9.0 ± 0.1	7.4 ± 0.1	0.8 ± 0.1	1.2 ± 0.0	1.4 ± 0.1
IM	426.2 ± 8.5	47.6 ± 1.9*	8.5 ± 0.1*	6.3 ± 0.1*	0.8 ± 0.1	1.3 ± 0.0	1.6 ± 0.2
Sheet	434.7 ± 9.8	53.5 ± 1.3*,**	8.2 ± 0.2*	5.8 ± 0.1*,**	0.9 ± 0.1	1.3 ± 0.0	1.4 ± 0.1
	HR (bpm)	LVEDP (mmHg)	LVDP (mmHg)	Max dP/dt (mmHg/s)	Min dP/dt (mmHg/s)	Contractility index	Tau (ms)
Catheterization							
Control	367.2 ± 4.1	15.0 ± 1.5	80.2 ± 2.1	6,808.8 ± 128.9	−5,425.4 ± 379.9	110.7 ± 2.6	18.4 ± 2.5
IM	374.4 ± 10.6	8.7 ± 1.5*	97.9 ± 3.1*	7,296.5 ± 100.7*	−6,658.3 ± 223.0*	115.2 ± 4.0	13.6 ± 0.4*
Sheet	388.2 ± 6.7	8.9 ± 0.6*	96.6 ± 2.3*	8,166.0 ± 185.9*,**	−7,455.3 ± 194.2*,**	128.9 ± 2.9*,**	13.0 ± 0.7*

Abbreviations: AWTd, end-diastolic anterior wall thickness; HR, heart rate; IM, intramyocardial injection; LV, left ventricle; LVDd, LV end-diastolic dimension; LVDP, LV developed pressure; LVDs, LV end-systolic dimension; LVEDP, LV end-diastolic pressure; LVEF, LV ejection fraction; MV E/A, mitral valve early/atrial velocity ratio; PWTd, end-diastolic posterior wall thickness.
n = 11–13 in echocardiography and n = 8–9 in cardiac catheterization. Data represented as mean ± SEM.
*P < 0.05 versus the Control group; **P < 0.05 versus the IM group.

machinery underlying such superiority of this approach remains ill-identified. There were preliminary data showing that the cell sheet technique achieved greater donor cell presence,[20] but these were not convincing enough to conclude whether this is because of increased initial retention, survival, or both of donor cells. In addition, regarding the paracrine effect, there is a concern that permeation of secreted factors from epicardially localized MSCs into the host myocardium might be blocked by the existing epicardium. Thus, we investigated the precise role of the cell sheet technique to augment the effects of MSC transplantation with particular focus on donor cell dynamics and paracrine effects.

RESULTS

Augmented improvement of postinfarction cardiac function by MSC sheet therapy

At day 28 post-treatment in a rat coronary artery ligation model, echocardiography showed that left ventricular ejection fraction post-myocardial infarction (MI) was significantly improved in the IM injection of MSC suspensions (IM group) compared with the Control (sham-treatment) group, and more importantly this improvement was further enhanced by the epicardial placement of an MSC sheet (Sheet group) (Table 1). In addition, post-treatment left ventricular end-systolic dimensions in the Sheet group were smaller than those in the Control and IM groups. Consistently, catheterization showed improved cardiac function (increased maximum and minimum dP/dt, and contractility index) in the Sheet group compared with the other groups (Table 1). These results confirmed that the use of the cell sheet technique improved the therapeutic effects of transplantation of bone marrow-derived MSCs for the treatment of MI in comparison with IM injection.

Improved initial retention, but not survival, of donor cells by MSC sheet therapy

To elucidate the donor cell dynamics that should be related to the enhanced therapeutic outcome by the cell sheet technique, we carried out serial, quantitative assessments of the donor cell presence. Of note, the Sheet group showed 6.4-fold increased initial retention of donor MSCs at 1 hour of transplantation (Figure 1a). This led to the greater donor cell presence in the Sheet group both persistently (at least until day 28).

Histological observations uncovered distinct donor cell distributions between the groups. In the IM group, donor cells formed localized clusters within the myocardium at 1 hour and 3 days (Figure 1b,c), which persisted up to day 28 with a reduced size (Figure 1d). In contrast, most of the donor cells remained on the epicardial surface in the Sheet group throughout the time studied (Figure 1e–g). It was noted that the thickness of the MSC sheets was enlarged between 1 hour and 3 days after placement (Figure 1e,f). However, this did not necessarily indicate that the donor cell presence was increased during this period, as donor MSCs in the sheets were more compacted and dense at 1 hour (**Supplementary Figure S1a–c**). It was speculated that compacted cells during the cell sheet generation had relaxed and become looser after epicardial placement, making the sheets to appear thicker at day 3, even though the number of donor MSCs presence was actually decreased (Figure 1a). Picrosirius red and hematoxylin staining showed that there was accumulation of extracellular collagen within the sheets at day 3, with an increasing tendency by day 28 (**Supplementary Figure S1d,e**). However, there was no sign of constrictive heart failure (left ventricular end-diastolic pressure was actually reduced in the Sheet group, compared with the Control group; Table 1).

Unexpectedly, the survival rates of donor cells calculated from the serial changes in donor cell presence (Figure 1a) were not improved in the Sheet group (61.4/94.8 = 0.65 (Sheet) versus 10.1/14.9 = 0.68 (IM) between 1 hour and 3 days, P = 0.81; 10.2/61.4 = 0.17 (Sheet) versus 2.9/10.1 = 0.29 (IM) between 3 and 28 days; P = 0.18). Consistent with this, the frequency of donor cell apoptosis was similar between the groups at day 3 (Figure 2).

Differentiation of donor cells after MSC sheet therapy

Immunohistostaining for cardiac troponin-T (cTnT) after transplantation of DiI-labeled MSCs did not detect clear evidence of cardiomyogenic differentiation of MSCs; there were no cells positive for both cTnT and DiI in the IM or Sheet group. Isolectin B4 staining detected a number of neovascular formations within

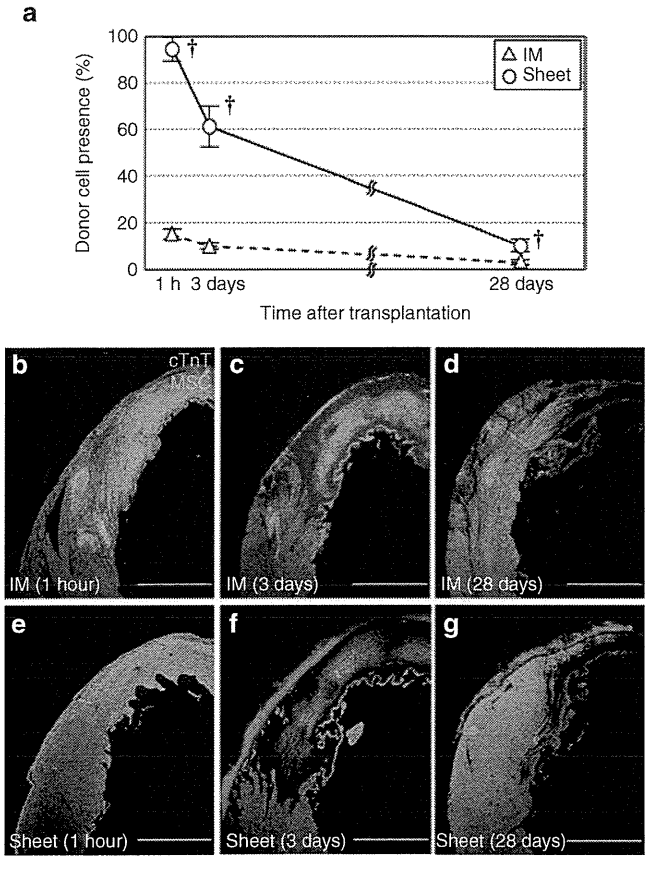

Figure 1 Improved donor cell retention and distribution by MSC sheet therapy. (**a**) Quantitative assessments by using the detection of the male-specific *sry* gene in the female heart showed that the initial retention (at 1 hour) and successive presence of donor cells (% of the total donor cell number grafted) were improved in the Sheet group compared with the IM group. †$P < 0.05$ versus the IM group, mean ± SEM for $n = 4–6$ in each point. Histological evaluation showed that donor cell distribution was distinct between groups; (**b–d**) intramyocardial cell cluster formation in the IM group (for 1 hour, days 3 and 28, respectively) versus (**e–g**) retention on the epicardial surface in the Sheet group (for 1 hour, days 3 and 28, respectively). Orange signal for MSCs (DiI); green for cTnT. Bar = 1 mm. cTnT, cardiac troponin-T; IM, intramyocardial injection; MSC, mesenchymal stromal cell.

the MSC sheets (Figure 3a–d). Most of these consisted of host-derived (DiI^-) endothelial cells, while the remaining contained donor-derived (DiI^+) cells, suggesting endothelial differentiation (or fusion) of donor MSCs, consistent to the previous findings.[21] However, in the host myocardium, there were no donor (DiI^+) MSC-containing vessels found.

Differentiation of donor MSCs to mesenchymal lineages, which was confirmed in our MSCs *in vitro* (**Supplementary Figure S2**), could be a concern if it occurs in the heart. However, our histological study showed that donor MSCs did not differentiate to adipocytes or osteocytes in the heart *in vivo* (**Supplementary Figure S3**), assuring the safety of MSC sheet therapy.

Findings to support the permeation of paracrine factors from MSC sheets into the heart

Given that the majority of donor cells were retained at the epicardial surface after MSC sheet therapy (Figure 1e–g), one

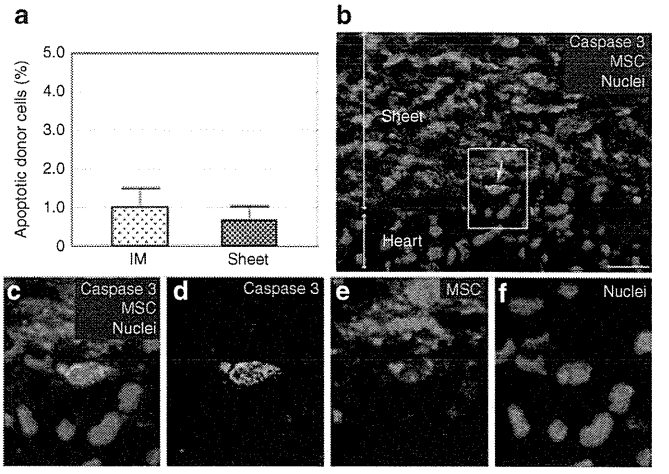

Figure 2 Donor cell apoptosis after MSC sheet therapy. (**a**) Immunolabeling for cleaved caspase-3 detected a similar frequency of apoptotic donor cells in both treatment groups at day 3. (**b**) A representative image of apoptotic donor cells (yellow arrow) after MSC sheet therapy is shown. Enlarged images of white-gated area in **b** are presented in **c–f** with each marker separate and merged. Green signal for cleaved caspase-3; orange for MSCs (DiI); blue for nuclei (DAPI). Bar = 30μm in **b**. DAPI, 4′,6-diamidino-2-phenylindole; IM, intramyocardial injection; MSC, mesenchymal stromal cell.

concern might be that the presence of the epicardium may inhibit the permeation of paracrine mediators from MSC sheets to the host myocardial tissues. Our study here provided several findings to ease it. First, after MSC sheet placement, the epicardium promptly regressed and disappeared. ICAM1 staining demonstrated the presence of the epicardial layer in the Control group (Figure 3e), while these $ICAM1^+$ epicardial cells were absent at both day 3 (Figure 3f) and day 28 (**Supplementary Figure S4a**) in the Sheet group. Second, isolectin B4 staining showed that many vasculatures formed within the MSC sheets were composed of host-derived (DiI^-) cells (Figure 3a–d), indicating migration of vascular cells from the host myocardium into the sheets. Third, CD31 staining detected host-derived (DiI^-) endothelial cells migrating into the MSC sheets by day 3, forming sprouting vessels from the host myocardium into the MSC sheet (Figure 3g). Fourth, there were donor MSCs, though relatively few in number, occasionally migrating into the host myocardium (Figure 3h and **Supplementary Figure S4b–e**). These findings collectively indicate that the epicardium disappeared shortly after MSC sheet placement, enabling early exchange of cells between the myocardium and MSC sheets, which could contribute to establishing vascular networks to feed the cell sheets. Such early establishment of communication between MSC sheets and myocardium assures permeation of molecules secreted from donor MSCs into the myocardium to facilitate the paracrine effect.

Improved paracrine effects: recovery of post-MI failing cardiac tissues by MSC sheet therapy

We then looked at histological evidence for the paracrine effects. At day 28, our picrosirius red staining showed that the infarct size in the Sheet group was the smallest among the three groups at day 28 (Figure 4a and **Supplementary Figure S5a–c**). This was associated with increase in the capillary density and reduction of

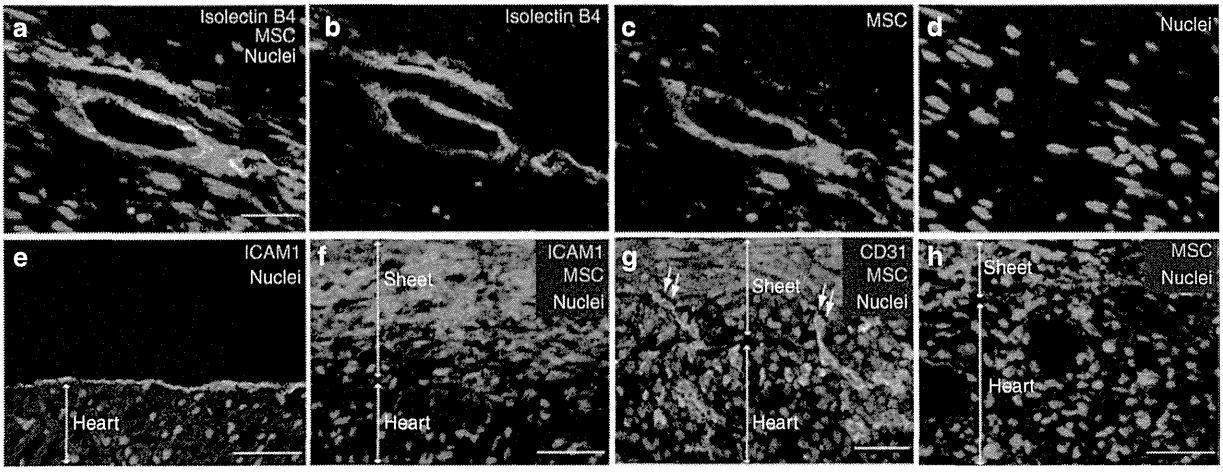

Figure 3 Donor cell behaviors and changes in the epicardium after MSC sheet therapy. (**a–d**) Isolectin B4 staining demonstrated that the vasculature in MSC sheets contained both host-derived (DiI^-) and donor MSC-derived (DiI^+) endothelial cells at day 28 after transplantation of DiI^+ sheets. (**e**) ICAM1 staining identified the epicardium in the Control group, (**f**) though this was absent by day 3 after MSC sheet therapy. (**g**) CD31 staining detected host-derived (DiI^-) endothelium sprouting into the MSC sheets at day 3. (**h**) The majority of donor MSCs retained on the surface of the heart (as in **f**), but a small number of MSCs had migrated into the host myocardium at day 3. Green signal for isolectin B4 in **a**,**b**, ICAM-1 in **e**,**f** or CD31 in **g**; orange for MSCs (DiI); blue for nuclei (DAPI). Bar = 30 μm in **a–d**, 50 μm in **e–h**. DAPI, 4′,6-diamidino-2-phenylindole; ICAM, intercellular adhesion molecule; MSC, mesenchymal stromal cell.

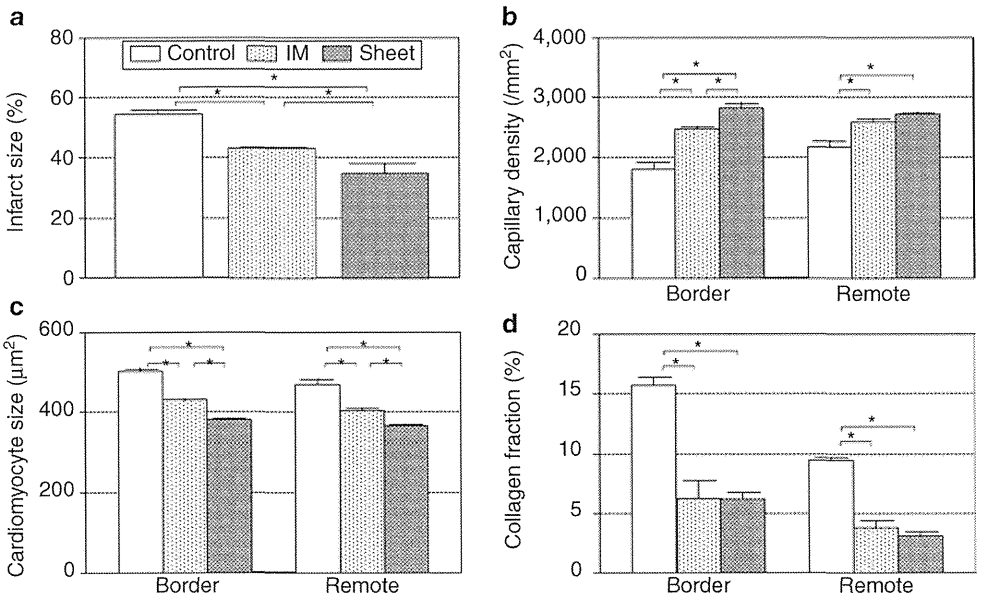

Figure 4 Histological recovery of post-MI failing cardiac tissues by MSC sheet therapy. (**a**) Histological studies detected reduced infarct size (**Supplementary Figure S5a–c**), (**b**) increased capillary density (**Supplementary Figure S5d–f**), (**c**) reduced cardiomyocyte hypertrophy (**Supplementary Figure S5g–i**), and (**d**) attenuated collagen deposition (**Supplementary Figure S5j–l**) at day 28 in the Sheet group compared with the Control group (and to the IM group in most points).*$P < 0.05$, mean ± SEM for $n = 4–5$ in each point. IM, intramyocardial injection; MI, myocardial infarction; MSC, mesenchymal stromal cell.

the cardiomyocyte hypertrophy in both border and remote areas in the Sheet group compared with other groups (Figure 4b,c and **Supplementary Figure S5d–i**). Extracellular collagen deposition in the Control group was markedly and widely attenuated in the Sheet and IM groups, with a slight tendency of further attenuation in the Sheet group (Figure 4d and **Supplementary Figure S5j–l**). These data suggest that both cell delivery methods achieved a similar pattern of paracrine effects to recover the failing myocardium post-MI, but the degree of the effects was more substantial after MSC sheet therapy compared with IM injection.

Improved paracrine effects: increased endogenous regeneration activity by MSC sheet therapy

Another target of the MSC-mediated paracrine effects is an activation of endogenous progenitor cells to regenerate cardiomyocytes and vasculature,[6,7] but this ability remains controversial.[22,23] Our *in vivo* studies added new information. The number of $Ki67^+$ proliferating cells markedly increased in both border and remote areas in the Sheet group at day 28, compared with the Control and IM groups (Table 2, Figure 5a–c, **Supplementary Figure S6a–d**). $Ki67^+$ cells were negative for CD45. In addition, the number of

Table 2 Endogenous regeneration by MSC sheet therapy

Cell number (/mm²)	Border			Remote		
	Control	IM	Sheet	Control	IM	Sheet
Total Ki67$^+$ cells	10.2 ± 1.6	17.7 ± 2.7	37.4 ± 4.0*,**	5.9 ± 1.3	10.9 ± 2.1	19.1 ± 3.0*,**
+ Isolectin B4$^+$	1.9 ± 0.8	4.7 ± 2.7	12.3 ± 2.7*,**	0.1 ± 0.1	2.6 ± 1.0	5.0 ± 2.1*
+ CD34$^+$	4.2 ± 1.1	10.7 ± 1.0*	23.0 ± 3.3*,**	4.2 ± 1.5	6.1 ± 1.2	16.4 ± 2.7*,**
+ Sca1$^+$	0.3 ± 0.3	0.5 ± 0.2	2.4 ± 0.2*,**	0.1 ± 0.1	0.2 ± 0.2	0.5 ± 0.2
+ cTnT$^+$	0.3 ± 0.2	0.3 ± 0.3	1.6 ± 0.7*	0	0	0
+ CD45$^+$	0.3 ± 0.2	0.2 ± 0.2*	0	0.1 ± 0.1	0	0.3 ± 0.2
Total Sca1$^+$ cells	1.8 ± 0.8	5.7 ± 1.0*	8.6 ± 1.5*	0.6 ± 0.3	1.0 ± 0.7	3.6 ± 1.1*,**

Abbreviations: cTnT, cardiac troponin-T; IM, intramyocardial injection; MSC, mesenchymal stromal cell.
The numbers of Ki67$^+$ proliferating cells, together with other relevant markers, and Sca-1$^+$ cells in border and infarct areas were assessed by immunohistolabeling at day 28. n = 4–5 in each point. Data represented as mean ± SEM.
*P < 0.05 versus the Control group; **P < 0.05 versus the IM group.

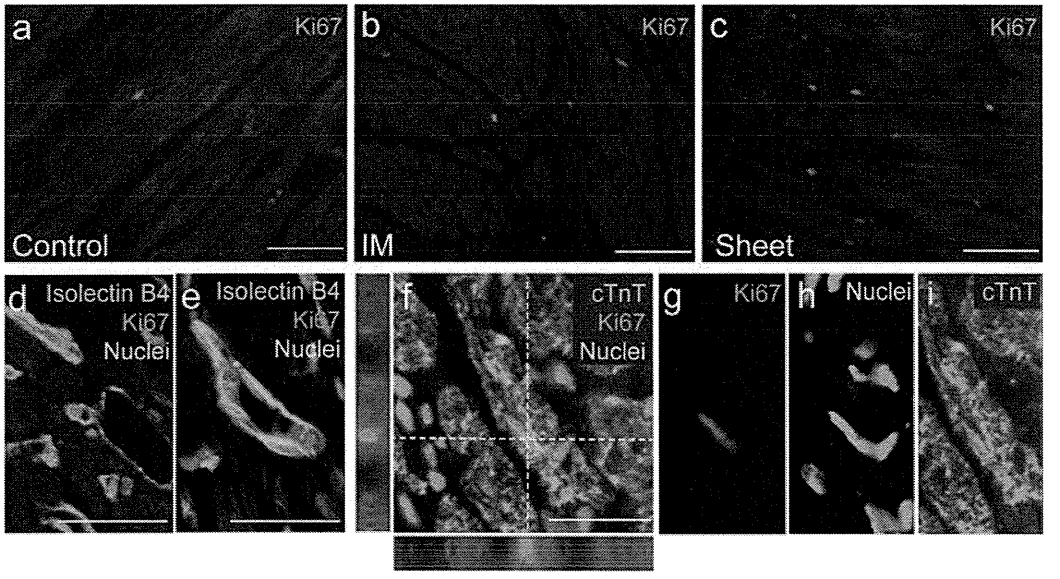

Figure 5 Improved endogenous regenerative activity by MSC sheet therapy. The number of Ki67$^+$ cells was increased in the Sheet group compared with the IM and Control groups. Representative images of Ki67$^+$ cells in the border areas of the (**a**) Control, (**b**) IM, and (**c**) Sheet groups at day 28 are shown (**Table 2**). Ki67$^+$/isolectin B4$^+$ cells were found in (**d**) capillaries as well as in (**e**) larger vessels after MSC sheet therapy. There were an increased number of Ki67$^+$/cTnT$^+$ proliferating cardiomyocytes in the Sheet group. (**f–i**) A representative image of Ki67$^+$/cTnT$^+$ cells after MSC sheet therapy is presented for each marker and merged. Green signal for isolectin B4 in **d,e**, cTnT in **f,i**; orange for Ki67; blue for nuclei (DAPI). Bar =100 μm in **a–c** and 30 μm in **d–f**. cTnT, cardiac troponin-T; DAPI, 4′,6-diamidino-2-phenylindole; IM, intramyocardial injection; MSC, mesenchymal stromal cell.

Sca-1$^+$/DiI$^-$ cells, which are reported to be cardiac progenitor cells,[24] as well as the number of Ki67$^+$/Sca-1$^+$/DiI$^-$ cells, were increased in the Sheet group.

It was found that most of Ki67$^+$ proliferating cells were also positive for isolectin B4 and/or CD34 (Table 2, Figure 5d,e, **Supplementary Figure S6e–h**), suggesting an acceleration of endogenous vascular regeneration. Ki67$^+$/isolectin B4$^+$ cells were found in capillaries (Figure 5d) as well as in larger vessels (Figure 5e). This enhanced vasculogenesis might contribute to the enhanced capillary density observed after MSC sheet therapy (Figure 4b). In addition, there were a small, but significantly increased, number of Ki67$^+$/cTnT$^+$ cells in the Sheet group, representing proliferating cardiomyocytes, compared with the Control group (Table 2 and Figure 5f–i). These cells were not donor (DiI$^+$)-derived and thus could be stemmed from differentiation of endogenous progenitor cells or from re-entry of host cardiomyocytes to the cell cycle. However, the number of these Ki67$^+$/cTnT$^+$ cells was not large enough to expect that they had contributed significantly to the improvement of cardiac function after MSC sheet therapy.

Amplified upregulation of paracrine mediators and signaling pathways by MSC sheet therapy

To gain a further insight into the augmented paracrine effects by MSC sheet therapy, we performed quantitative reverse transcription-PCR screening for genes presumed to be relevant to the MSC-mediated paracrine effects.[2,3,21,24–29] As a result, we observed that myocardial expression of *IL-10*, *VCAM-1*, *TIMP-1*, *IGF-1*, *MMP-2*, *HIF1-α*, *SDF-1*, *MMP-9*, and *bFGF* was upregulated in the Sheet group at day 3 compared with the Control group (Figure 6). These data corresponded well with the above-discussed histological changes in neovascular formation, fibrosis, and endogenous myocardial regeneration (Figures 4 and 5). Of note, upregulation

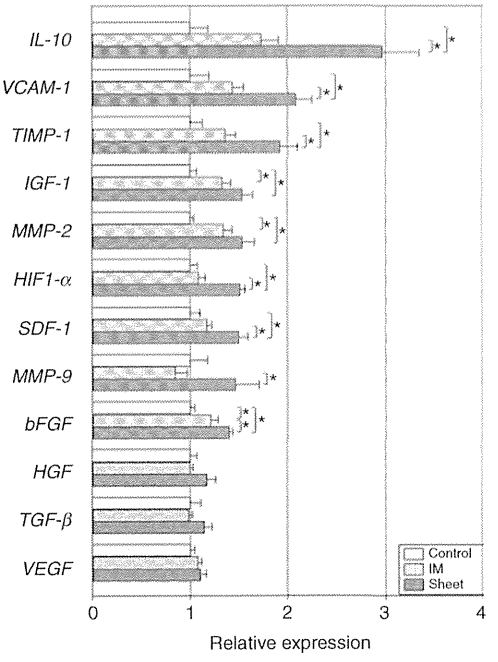

Figure 6 Amplified upregulation of paracrine effect-relevant genes by MSC sheet therapy. Quantitative RT-PCR screening detected upregulation of a group of genes likely to be relevant to the MSC-derived paracrine effects in the Sheet group, and in the IM group to a lesser extent, at day 3. All expression levels were normalized to that in the Control group, which was assigned a value of 1.0. $*P < 0.05$, mean ± SEM for $n = 5$–6 in each group. IM, intramyocardial injection; MSC, mesenchymal stromal cell; RT-PCR, reverse transcription-PCR.

of these genes was also observed in the IM group, but to a lesser extent compared with the Sheet group. Major signaling pathways relevant to the observed histological changes[22,23] have also shown the same trend; JNK and p38 MAPK were both activated at day 3 in the Sheet and IM groups, with more substantial activation in the Sheet group, as compared with the Control group (**Supplementary Figure S7**). Of note, this amplified upregulation of paracrine-related genes and signaling pathways after MSC sheet therapy matched with both the above-mentioned increase in donor cell presence and augmented paracrine benefits. Upregulation of most of these genes was, however, reduced to the baseline (values in the Control group) by day 28 after MSC sheet therapy (**Supplementary Figure S8**), corresponding with the largely reduced donor cell presence by this time (Figure 1a).

DISCUSSION

This translational study has, for the first time, validated that the epicardial placement of bone marrow-derived MSC-sheets is feasible, safe, and more effective in treating heart failure, compared with IM MSC injection. As a primary factor responsible for the superiority of the cell sheet technique, we identified the improved initial retention of donor MSCs. Soon after epicardial placement, MSC sheets were found to firmly adhere to the heart probably due to the preserved extracellular matrix underlying the cell sheets, achieving 6.4-fold higher initial retention of MSCs, compared with IM injection of MSC suspensions. Even though the successive donor cell survival rate was not increased, this improved initial retention was substantial enough to achieve the significant increase of donor cell presence for at least 28 days. Importantly, this effect was robust enough to amplify the paracrine effects to recover the post-MI failing myocardium and to augment functional recovery of the hearts. Observed paracrine effects included the increase in neovascular formation, decrease in fibrosis, attenuation of cardiomyocyte hypertrophy, and improvement of endogenous myocardial regeneration. Underpinning these changes, there was amplified myocardial upregulation of a group of relevant molecules and related signaling pathways after MSC sheet therapy compared with IM injection.

In addition, we observed that the epicardium disappeared shortly after MSC sheet placement with establishment of early communication between the sheets and host myocardium, suggesting that the pre-existing epicardium did not hinder the permeation of molecules secreted from donor MSCs into the myocardium to facilitate the paracrine effect. As regards differentiation of donor MSCs, we observed donor cell-derived endothelial cells within the sheets (but not in the host myocardium), while there was no finding suggesting myogenic differentiation.

Recent research has shed light on the ability of MSCs to stimulate endogenous progenitor cells towards cardiomyocyte regeneration in a paracrine manner.[6,7] However, this effect after IM MSC injection remains debated.[22,23] Here, our study provided new evidence to understand this event. MSC sheet therapy enhanced cardiomyogenic regeneration *via* an endogenous route, compared with the sham control, in association with upregulation of *IGF-1* and *SDF-1*, both of which are known to increase recruitment and/or activation of endogenous stem/progenitor cells.[27–29] In contrast, the regenerative activity was much less extensive after IM MSC injection, corresponding to lower upregulation of *SDF-1*. These data collectively suggest that MSCs do have a capability to stimulate endogenous cardiomyogenic regeneration, and that the extent of MSC presence after IM injection may not be sufficient to activate this pathway. While on the other hand, the cell sheet technique achieved the markedly increased presence of MSCs, which would enable the production of a necessary magnitude of paracrine stimuli for regeneration. Having said this, cardiomyocyte regeneration even after MSC sheet therapy was not extensive enough to influence the global cardiac function. Further refinement is needed to realize therapeutic myocardial regeneration based on MSC-mediated paracrine effects.

Our quantitative data of donor cell presence demonstrated that the survival rate of grafted MSCs after the cell sheet technique was so low that ~90% of the initially retained MSCs were dead or disappeared by day 28. Corresponding to this, the myocardial upregulation of paracrine effect-related genes after MSC sheet therapy diminished by day 28. However, despite these, cardiac function and structure were improved for at least 28 days. This let us speculate that the contribution of the paracrine factors would take place mainly during the early phase after MSC sheet therapy, and this is sufficient to initiate long-lasting changes in the cardiac tissue components (*i.e.*, neovascular formation, reduced fibrosis, attenuation of cardiomyocyte hypertrophy, and endogenous myocardial regeneration) and resultant recovery of global cardiac function. Then, once established, the improved cardiac function could last for a longer time.

It was unexpected that donor cell survival was not improved by the cell sheet technique compared with IM injection. There was

apoptosis in donor cells in the sheet to the same ratio to IM injection. We speculate that cell death in the sheet could be caused by relative hypoxia and/or insufficient nutrition. There was increased neovascular formation within the host myocardium and vessel formation within the sheets. However, the donor cells are likely to die before the neovascular formation is functionally complete enough for supply to the sheet. In addition, there were sprouting vessels from the myocardium to the sheets (Figure 3g); however, the extent of these connecting vessels did not appear to be sufficient. These would collectively result in inadequate oxygen/nutrition delivery to donor cells and inhibiting long-term survival of donor cells. In order to improve donor cell survival after cell sheet technique, we believe it is important to further improve vascular formation in the sheets and vascular connections between the host myocardium and sheets for enhancing perfusion of the sheets. This might be achieved by co-treatment with angiogenesis factors such as HGF[30] or cotransplantation with endothelial cells or endothelial progenitor cells.[31,32]

A limitation of the present study may be that IM cell injection was carried out into two sites in a heart. Although this is one of the most frequently used, standard protocols for IM cell injection in rat,[11,33,34] we cannot deny a possibility that an increase in the number of IM injections might enhance the therapeutic efficacy.

In conclusion, the cell sheet technique enhanced initial retention and following presence of bone marrow-derived MSCs, amplified subsequent paracrine effects to recover/regenerate the damaged heart, and improved therapeutic outcomes, compared with IM injection. This timely information will provide important clinical implication to refine MSC-based therapy that has recently entered clinical trials. As the cell sheet placement requires open chest procedures, it would be a reasonable idea to carry out MSC sheet therapy in conjunction with routine cardiac surgery, like coronary artery bypass grafting, left ventricular assist device implantation, and so on. Further preclinical investigations on the safety and efficiency of MSC sheet therapy are warrantied for enabling early clinical application of this promising approach.

MATERIALS AND METHODS

All studies were performed with the approval of the institutional ethics committee and the Home Office, UK. The investigation conforms to the Principles of Laboratory Animal Care formulated by the National Society for Medical Research and the Guide for the Care and Use of Laboratory Animals (US National Institutes of Health Publication, 1996). All *in vivo* and *in vitro* assessments were carried out in a blinded manner. Please see the **Supplementary Materials and Methods** for additional details.

Generation of MSC suspensions and MSC sheets. MSCs were isolated from the bone marrow from the tibias and femurs of male Lewis rats (100–150 g; Charles River Laboratories, Margate, UK) as described previously[35] and characterized (**Supplementary Figure S2**). To generate an MSC sheet, 4×10^6 MSCs were seeded at passages 3–5 on a 35 mm temperature-responsive culture dish (UpCell; CellSeed, Tokyo, Japan). Following incubation for 12 hours at 37 °C under 5% CO_2, the culture temperature was lowered to 20–22 °C enabling the MSC sheet to detach from the dish.[15] The collected MSC sheets were 12–15 mm in diameter. For injection, 4×10^6 MSCs were collected using trypsinization and suspended in 200 µl phosphate-buffered saline. Cell number counting by digesting a sheet with trypsin demonstrated that a freshly generated MSC sheet contained $4.1 \pm 0.2 \times 10^6$ cells ($n = 5$), assuring that there was no difference in the MSC number between cell sheet and IM injection groups. For graft tracking studies, MSCs were labeled with CM-DiI (DiI; Molecular Probes, Paisley, UK) according to the manufacturer's protocol.

Animal models. Female Lewis rats (150–200 g; Charles River Laboratories) underwent left coronary artery ligation to generate MI as described previously.[11] The animals were randomly assigned to undergo transplantation of 4×10^6 MSCs from syngeneic male rats by either Sheet group or IM group. For the Sheet group, an MSC sheet was placed to cover the infarct and surrounding border areas. After epicardial placement, MSC sheets were found to stably adhere to the heart within 20–30 minutes. For the IM group, MSCs suspended in 200 µl phosphate-buffered saline were intramyocardially injected with a 31G needle into two sites (100 µl each), targeting the border and infracted areas. Sham-treated (MI only) rats served as the Control group.

Cardiac performance measurement. Cardiac function and dimensions, and hemodynamic parameters were measured by using echocardiography (Vevo-770; VisualSonics, Amsterdam, The Netherlands) and catheterization (SPR-320 and PVAN3.2; Millar Instruments, Houston, TX) under general anesthesia using isoflurane inhalation in a blinded manner by well-experienced staff as previously described.[11,36,37] All data were collected from at least three different measurements and averaged.

Quantitative assessment of donor cell presence. DNA was extracted from the whole left ventricular walls and the presence of male cells in the female hearts was quantitatively assessed to define donor cell presence/survival using real-time PCR (Prism 7900HT; Applied Biosystems, Paisley, UK) for the Y-chromosome-specific *sry* gene as previously described.[36]

Histological analysis. At chosen time points, the hearts were excised, fixed with 4% paraformaldehyde, and frozen. Cryosections were cut and incubated with polyclonal anti-cTnT antibody (1:200 dilution; HyTest, Turku, Finland), polyclonal anti-cleaved caspase-3 antibody (1:250; Cell Signaling Technology, Danvers, MA), biotin-conjugated Griffonia simplicifolia lectin I-isolectin B_4 (1:100; Vector Laboratories, Peterborough, UK), monoclonal anti-CD45 antibody (1:50; BD, Oxford, UK), monoclonal anti-CD11b antibody (1:50; Chemicon, Watford, UK), monoclonal anti-granulocyte antigen antibody (1:20; AbD Serotec, Kidlington, UK), monoclonal anti-OX62 antibody (1:25; AbD Serotec), polyclonal anti-CD3 antibody (1:100; Abcam, Cambridge, UK), polyclonal anti-CD34 antibody (1:700; R&D, Abingdon, UK), monoclonal anti-CD31 antibody (1:50; AbD Serotec), monoclonal anti-ICAM1 antibody (1:50; Abcam), monoclonal anti-Ki67 antibody (1:50; Dako, Cambridgeshire, UK), or polyclonal anti-Sca-1 antibody (1:25; Abnova, Heidelberg, Germany) followed by visualization using fluorophore-conjugated secondary antibodies (Molecular Probes). Sections were analyzed by fluorescence microscopy (BZ8000; Keyence, Milton Keynes, UK) with or without nuclear counterstaining using 4′,6-diamidino-2-phenylindole (DAPI). Ten different fields from each of the border and remote areas per heart were randomly selected and assessed. Another set of sections were stained with 0.1% picrosirius red for assessing infarct size (% of scar length to total left ventricular circumference) and for detecting collagen deposition using NIH image-analysis software.[11,36] To evaluate the cardiomyocyte size, the cross-sectional area of appropriately detected cardiomyocytes (transversely cut; having central nuclei and surrounded by circle-shaped capillaries)[37] was measured for 50 cardiomyocytes per area. In addition, for detecting adipogenic and osteogenic differentiation, staining with Oil red O and Alizarin red was performed as above.[38–40]

Analysis of myocardial gene expression and signaling pathway activation. Total RNA was extracted from the whole left ventricular walls and assessed for myocardial gene expression by quantitative reverse transcription-PCR (Prism 7900HT) as previously described.[36] TaqMan primers and probes were purchased from Applied Biosystems. Expression was

normalized using *Ubiquitin C*. In addition, protein was extracted and assessed by western blotting. Primary antibodies were obtained from Cell Signaling Technology; anti-phosphorylated ERK1/2 (#4377), phosphorylated JNK (#9251), phosphorylated p38 (#9216), phosphorylated Akt (#4051), and phosphorylated PI3K (#4228). The labeled membrane was stripped, and then re-probed with anti-ERK1/2 (#9102), JNK (#9252), p38 (#9212), Akt (#9272), PI3K (#4292) antibodies. Blots were imaged and quantitative analysis was performed using Alpha view software (Alpha Innotech, Santa Clara, CA).[36]

Statistical analysis. All values are expressed as mean ± SEM. Statistical comparison of the data was performed using the Student's unpaired *t*-test for the analysis of donor cell apoptosis. All other data were statistically analyzed with one-way analysis of variance followed by Fisher's post-hoc analysis to compare groups. A value of $P < 0.05$ was considered statistically significant.

SUPPLEMENTARY MATERIAL

Figure S1. Supplementary histological findings to **Figure 1** (Less densely packed donor cells in the MSC sheets after epicardial placement).
Figure S2. *In vitro* characterization of rat bone marrow-derived MSCs.
Figure S3. Adipogenic and osteogenic differentiation of MSCs *in vivo*.
Figure S4. Supplementary histological findings to **Figure 3** (Donor cell behaviors and changes in the epicardium after MSC sheet therapy).
Figure S5. Supplementary histological findings to **Figure 4** (Histological recovery of post-MI failing cardiac tissues by MSC sheet therapy).
Figure S6. Supplementary histological findings to **Figure 5** and **Table 2** (Improved endogenous regeneration activity by MSC sheet therapy).
Figure S7. Elevated activation of paracrine effect-related signal pathways by MSC sheet therapy.
Figure S8. Supplementary data to **Figure 6** (Myocardial gene expression at day 28 after MSC sheet therapy).
Materials and Methods.

ACKNOWLEDGMENTS

This research forms of the research themes contributing to the translational research portfolio of Barts Cardiovascular Biomedical Research Unit which is supported and funded by the UK National Institute of Health Research (New and Emerging Applications of Technology Progarmme (NEAT L018) and the Barts and The London Charity (ETHG1B8R)). The authors declared no conflict of interest.

REFERENCES

1. Menasche, P (2011). Cardiac cell therapy: lessons from clinical trials. *J Mol Cell Cardiol* **50**: 258–265.
2. Passier, R, van Laake, LW and Mummery, CL (2008). Stem-cell-based therapy and lessons from the heart. *Nature* **453**: 322–329.
3. Choi, YH, Kurtz, A and Stamm, C (2011). Mesenchymal stem cells for cardiac cell therapy. *Hum Gene Ther* **22**: 3–17.
4. Boyle, AJ, McNiece, IK and Hare, JM (2010). Mesenchymal stem cell therapy for cardiac repair. *Methods Mol Biol* **660**: 65–84.
5. Gnecchi, M, He, H, Liang, OD, Melo, LG, Morello, F, Mu, H *et al.* (2005). Paracrine action accounts for marked protection of ischemic heart by Akt-modified mesenchymal stem cells. *Nat Med* **11**: 367–368.
6. Hatzistergos, KE, Quevedo, H, Oskouei, BN, Hu, Q, Feigenbaum, GS, Margitich, IS *et al.* (2010). Bone marrow mesenchymal stem cells stimulate cardiac stem cell proliferation and differentiation. *Circ Res* **107**: 913–922.
7. Nakanishi, C, Yamagishi, M, Yamahara, K, Hagino, I, Mori, H, Sawa, Y *et al.* (2008). Activation of cardiac progenitor cells through paracrine effects of mesenchymal stem cells. *Biochem Biophys Res Commun* **374**: 11–16.
8. <http://clinicaltrials.gov/>. 4 September 2012.
9. Suzuki, K, Murtuza, B, Beauchamp, JR, Brand, NJ, Barton, PJ, Varela-Carver, A *et al.* (2004). Role of interleukin-1beta in acute inflammation and graft death after cell transplantation to the heart. *Circulation* **110** (suppl. 1): II219–224.
10. Suzuki, K, Murtuza, B, Beauchamp, JR, Smolenski, RT, Varela-Carver, A, Fukushima, S *et al.* (2004). Dynamics and mediators of acute graft attrition after myoblast transplantation to the heart. *FASEB J* **18**: 1153–1155.
11. Fukushima, S, Varela-Carver, A, Coppen, SR, Yamahara, K, Felkin, LE, Lee, J *et al.* (2007). Direct intramyocardial but not intracoronary injection of bone marrow cells induces ventricular arrhythmias in a rat chronic ischemic heart failure model. *Circulation* **115**: 2254–2261.
12. Yang, J, Yamato, M, Kohno, C, Nishimoto, A, Sekine, H, Fukai, F *et al.* (2005). Cell sheet engineering: recreating tissues without biodegradable scaffolds. *Biomaterials* **26**: 6415–6422.
13. Elloumi-Hannachi, I, Yamato, M and Okano, T (2010). Cell sheet engineering: a unique nanotechnology for scaffold-free tissue reconstruction with clinical applications in regenerative medicine. *J Intern Med* **267**: 54–70.
14. Suzuki, K, Brand, NJ, Smolenski, RT, Jayakumar, J, Murtuza, B and Yacoub, MH (2000). Development of a novel method for cell transplantation through the coronary artery. *Circulation* **102** (suppl. 3): III359–III364.
15. Miyahara, Y, Nagaya, N, Kataoka, M, Yanagawa, B, Tanaka, K, Hao, H *et al.* (2006). Monolayered mesenchymal stem cells repair scarred myocardium after myocardial infarction. *Nat Med* **12**: 459–465.
16. Memon, IA, Sawa, Y, Fukushima, N, Matsumiya, G, Miyagawa, S, Taketani, S *et al.* (2005). Repair of impaired myocardium by means of implantation of engineered autologous myoblast sheets. *J Thorac Cardiovasc Surg* **130**: 1333–1341.
17. Matsuura, K, Honda, A, Nagai, T, Fukushima, N, Iwanaga, K, Tokunaga, M *et al.* (2009). Transplantation of cardiac progenitor cells ameliorates cardiac dysfunction after myocardial infarction in mice. *J Clin Invest* **119**: 2204–2217.
18. Bel, A, Planat-Bernard, V, Saito, A, Bonnevie, L, Bellamy, V, Sabbah, L *et al.* (2010). Composite cell sheets: a further step toward safe and effective myocardial regeneration by cardiac progenitors derived from embryonic stem cells. *Circulation* **122** (suppl. 11): S118–S123.
19. Wagner, W, Wein, F, Seckinger, A, Frankhauser, M, Wirkner, U, Krause, U *et al.* (2005). Comparative characteristics of mesenchymal stem cells from human bone marrow, adipose tissue, and umbilical cord blood. *Exp Hematol* **33**: 1402–1416.
20. Sekiya, N, Matsumiya, G, Miyagawa, S, Saito, A, Shimizu, T, Okano, T *et al.* (2009). Layered implantation of myoblast sheets attenuates adverse cardiac remodeling of the infarcted heart. *J Thorac Cardiovasc Surg* **138**: 985–993.
21. Oswald, J, Boxberger, S, Jørgensen, B, Feldmann, S, Ehninger, G, Bornhäuser, M *et al.* (2004). Mesenchymal stem cells can be differentiated into endothelial cells *in vitro*. *Stem Cells* **22**: 377–384.
22. Loffredo, FS, Steinhauser, ML, Gannon, J and Lee, RT (2011). Bone marrow-derived cell therapy stimulates endogenous cardiomyocyte progenitors and promotes cardiac repair. *Cell Stem Cell* **8**: 389–398.
23. Cho, J, Zhai, P, Maejima, Y and Sadoshima, J (2011). Myocardial injection with GSK-3ß-overexpressing bone marrow-derived mesenchymal stem cells attenuates cardiac dysfunction after myocardial infarction. *Circ Res* **108**: 478–489.
24. Oh, H, Bradfute, SB, Gallardo, TD, Nakamura, T, Gaussin, V, Mishina, Y *et al.* (2003). Cardiac progenitor cells from adult myocardium: homing, differentiation, and fusion after infarction. *Proc Natl Acad Sci USA* **100**: 12313–12318.
25. Burchfield, JS, Iwasaki, M, Koyanagi, M, Urbich, C, Rosenthal, N, Zeiher, AM *et al.* (2008). Interleukin-10 from transplanted bone marrow mononuclear cells contributes to cardiac protection after myocardial infarction. *Circ Res* **103**: 203–211.
26. Huang, Y, Hickey, RP, Yeh, JL, Liu, D, Dadak, A, Young, LH *et al.* (2004). Cardiac myocyte-specific HIF-1alpha deletion alters vascularization, energy availability, calcium flux, and contractility in the normoxic heart. *FASEB J* **18**: 1138–1140.
27. Askari, AT, Unzek, S, Popovic, ZB, Goldman, CK, Forudi, F, Kiedrowski, M *et al.* (2003). Effect of stromal-cell-derived factor 1 on stem-cell homing and tissue regeneration in ischaemic cardiomyopathy. *Lancet* **362**: 697–703.
28. Haider, HKh, Jiang, S, Idris, NM and Ashraf, M (2008). IGF-1-overexpressing mesenchymal stem cells accelerate bone marrow stem cell mobilization via paracrine activation of SDF-1alpha/CXCR4 signaling to promote myocardial repair. *Circ Res* **103**: 1300–1308.
29. Santini, MP, Tsao, L, Monassier, L, Theodoropoulos, C, Carter, J, Lara-Pezzi, E *et al.* (2007). Enhancing repair of the mammalian heart. *Circ Res* **100**: 1732–1740.
30. Siltanen, A, Kitabayashi, K, Lakkisto, P, Mäkelä, J, Pätilä, T, Ono, M *et al.* (2011). hHGF overexpression in myoblast sheets enhances their angiogenic potential in rat chronic heart failure. *PLoS ONE* **6**: e19161.
31. Sekine, H, Shimizu, T, Hobo, K, Sekiya, S, Yang, J, Yamato, M *et al.* (2008). Endothelial cell coculture within tissue-engineered cardiomyocyte sheets enhances neovascularization and improves cardiac function of ischemic hearts. *Circulation* **118** (suppl. 14): S145–S152.
32. Asakawa, N, Shimizu, T, Tsuda, Y, Sekiya, S, Sasagawa, T, Yamato, M *et al.* (2010). Pre-vascularization of *in vitro* three-dimensional tissues created by cell sheet engineering. *Biomaterials* **31**: 3903–3909.
33. Mazo, M, Cemborain, A, Gavira, JJ, Abizanda, G, Araña, M, Casado, M *et al.* (2012). Adipose stromal vascular fraction improves cardiac function in chronic myocardial infarction through differentiation and paracrine activity. *Cell Transplant* **21**: 1023–1037.
34. Kim, SH, Moon, HH, Kim, HA, Hwang, KC, Lee, M and Choi, D (2011). Hypoxia-inducible vascular endothelial growth factor-engineered mesenchymal stem cells prevent myocardial ischemic injury. *Mol Ther* **19**: 741–750.
35. Hayashi, Y, Tsuji, S, Tsujii, M, Nishida, T, Ishii, S, Iijima, H *et al.* (2008). Topical transplantation of mesenchymal stem cells accelerates gastric ulcer healing in rats. *Am J Physiol Gastrointest Liver Physiol* **294**: G778–G786.
36. Shintani, Y, Fukushima, S, Varela-Carver, A, Lee, J, Coppen, SR, Takahashi, K *et al.* (2009). Donor cell-type specific paracrine effects of cell transplantation for post-infarction heart failure. *J Mol Cell Cardiol* **47**: 288–295.
37. Litwin, SE, Raya, TE, Anderson, PG, Litwin, CM, Bressler, R and Goldman, S (1991). Induction of myocardial hypertrophy after coronary ligation in rats decreases ventricular dilatation and improves systolic function. *Circulation* **84**: 1819–1827.
38. Jaiswal, N, Haynesworth, SE, Caplan, AI and Bruder, SP (1997). Osteogenic differentiation of purified, culture-expanded human mesenchymal stem cells *in vitro*. *J Cell Biochem* **64**: 295–312.
39. Rochefort, GY, Delorme, B, Lopez, A, Hérault, O, Bonnet, P, Charbord, P *et al.* (2006). Multipotential mesenchymal stem cells are mobilized into peripheral blood by hypoxia. *Stem Cells* **24**: 2202–2208.
40. Breitbach, M, Bostani, T, Roell, W, Xia, Y, Dewald, O, Nygren, JM *et al.* (2007). Potential risks of bone marrow cell transplantation into infarcted hearts. *Blood* **110**: 1362–1369.

Muscle-derived Stem Cell Sheets Support Pump Function and Prevent Cardiac Arrhythmias in a Model of Chronic Myocardial Infarction

Naosumi Sekiya[1–3], Kimimasa Tobita[2,4], Sarah Beckman[1], Masaho Okada[1,5], Burhan Gharaibeh[1,2,6], Yoshiki Sawa[7], Robert L Kormos[2,3] and Johnny Huard[1,2,6]

[1]*Stem Cell Research Center, University of Pittsburgh, Pittsburgh, Pennsylvania, USA;* [2]*McGowan Institute for Regenerative Medicine, University of Pittsburgh, Pittsburgh, Pennsylvania, USA;* [3]*Department of Cardiovascular Surgery, University of Pittsburgh, Pittsburgh, Pennsylvania, USA;* [4]*Department of Developmental Biology, University of Pittsburgh, Pittsburgh, Pennsylvania, USA;* [5]*Department of Cardiothoracic Surgery, Nagoya University Graduate School of Medicine, Nagoya, Japan;* [6]*Department of Orthopaedic Surgery, University of Pittsburgh, Pittsburgh, Pennsylvania, USA;* [7]*Department of Cardiovascular Surgery, Osaka University Graduate School of Medicine, Osaka, Japan*

Direct intracardiac cell injection for heart repair is hindered by numerous limitations including: cell death, poor spreading of the injected cells, arrhythmia, needle injury, etc. Tissue-engineered cell sheet implantation has the potential to overcome some of these limitations. We evaluated whether the transplantation of a muscle-derived stem cell (MDSC) sheet could improve the regenerative capacity of MDSCs in a chronic model of myocardial infarction. MDSC sheet-implanted mice displayed a reduction in left ventricle (LV) dilation and sustained LV contraction compared with the other groups. The MDSC sheet formed aligned myotubes and produced a significant increase in capillary density and a reduction of myocardial fibrosis compared with the other groups. Hearts transplanted with the MDSC sheets did not display any significant arrhythmias and the donor MDSC survival rate was higher than the direct myocardial MDSC injection group. MDSC sheet implantation yielded better functional recovery of chronic infarcted myocardium without any significant arrhythmic events compared with direct MDSC injection, suggesting this cell sheet delivery system could significantly improve the myocardial regenerative potential of the MDSCs.

Received 21 March 2012; accepted 26 November 2012; advance online publication 15 January 2013. doi:10.1038/mt.2012.266

INTRODUCTION

Cardiovascular disease is one of the major causes of death worldwide. Ischemic injury and chronic cardiomyopathy lead to permanent loss of cardiac contractile tissue and ultimately heart failure and death. As a promising therapy, cellular cardiomyoplasty (CCM) has been widely investigated, and researchers are working to identify suitable donor cells that can be used to improve cardiac function after injury and disease. The most promising populations evaluated to date include skeletal myoblasts,[1,2] murine embryonic stem cells,[3,4] bone marrow-derived mesenchymal stem cells,[5–7] purified (enriched) hematopoietic stem cells,[8,9] blood- and bone marrow-derived endothelial progenitor cells,[10,11] and cardiac stem cells.[12,13] Each of the donor cell populations mentioned above has demonstrated some beneficial effects when injected into the heart, but various ethical, biologic, and technical concerns limit their suitability for use in human patients.

Skeletal myoblasts have been extensively investigated as a therapeutic cell source for heart regeneration. However, numerous limitations have hindered the overall application of myoblast transplantation for cardiac repair such as: poor cell survival, limited dissemination/spreading of the cells at the site of injury, immune responses, etc. In addition, arrhythmias after autologous myoblast injection have been observed and consequently the implantation of an intracardiac defibrillator has often been required for patients enrolled in myoblast transplantation trials for cardiac repair.[14] The prevalence of arrhythmias after cell injection has prompted investigators to consider other cell delivery methods for cardiac repair.[15] These include direct intramuscular injection, intravascular cell administration,[16] cells seeded onto a polymer (patch),[17] or cell sheets, such as the one used in the present study.

Tissue-engineered cell sheet transplantation seems to overcome some of the limitations over conventional cell injection including: (i) the elimination of trypsin to detach the cells from the culture dishes, (ii) the elimination of direct needle injury to the already compromised heart, and (iii) the ability to cover a larger infarction area due to an increased survival of the transplanted cells.[18,19]

Muscle-derived stem cells (MDSCs) are isolated from skeletal muscle *via* a modified preplate technique based on their adhesion to collagen-coated flasks.[20] MDSCs are less committed to the myogenic lineage than myoblasts and have the capacity for long-term proliferation and can differentiate to various lineages such as bone, cartilage, and nerve.[21,22] MDSCs express lower levels of Pax7 and desmin than myoblasts but will express fast skeletal myosin heavy chain (fsMHC) upon differentiation into myotubes and muscle fibers.[23] Our previous studies have shown that MDSCs repair the infarcted heart in a more effective manner than conventional

Correspondence: *Johnny Huard, Stem Cell Research Center, 450 Technology Drive, Bridgeside Point II, Pittsburgh, Pennsylvania 15219, USA. E-mail: jhuard@pitt.edu*

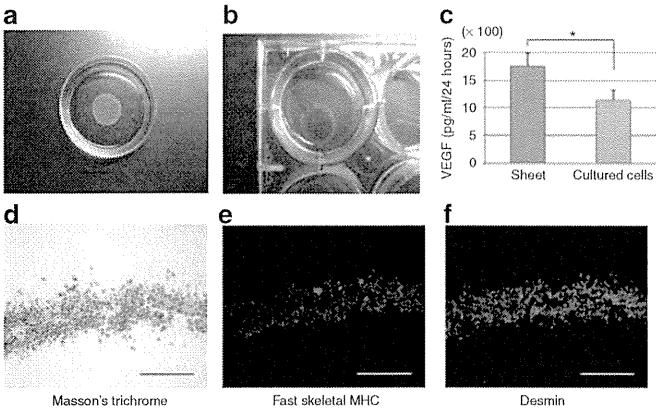

Figure 1 MDSC sheet construction. (**a**) Five million MDSCs were seeded on 3.5 cm temperature-responsive dish. (**b**) LacZ gene-transduced MDSC sheet (X-gal stain). (**c**) Higher expression of VEGF from MDSC sheet when compared with dissociated cultured cells. (VEGF (pg/ml/24 hours), ELISA, $*P < 0.05$). (**d–f**) Cross-section of MDSC sheet, stained by (**d**) Masson's trichrome, (**e**) fast skeletal MHC (MY-32), and (**f**) desmin staining; bar = 200 μm. MDSC, muscle-derived stem cell; MHC, myosin heavy chain; VEGF, vascular endothelial growth factor.

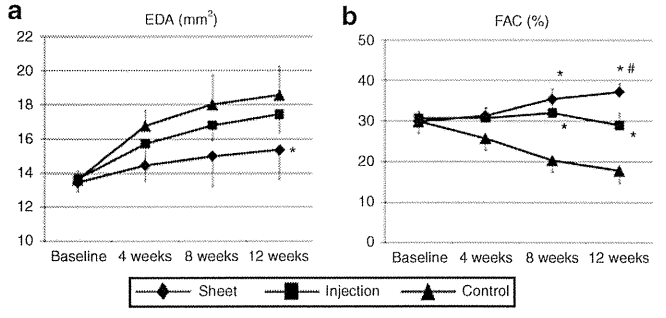

Figure 2 Cardiac function. (**a**) The dilation of left ventricle end diastolic area (EDA) was significantly improved in the sheet group at 12 weeks, compared with control (sham) group. (**b**) Both the sheet and injection groups had greater left ventricle contractility, as measured by fractional area change (FAC) at 8 and 12 weeks after transplantation when compared with the control group. Moreover, 12 weeks after, the FAC of the sheet group was significantly improved when compared with the other two groups. For the sheet group at baseline $n = 4$, at 4 weeks $n = 9$, at 8 weeks $n = 5$, at 12 weeks $n = 5$. For the injection group at baseline $n = 7$, at 4 weeks $n = 7$, at 8 weeks $n = 5$, at 12 weeks $n = 5$. For the control/sham group at baseline $n = 7$, at 4 weeks $n = 7$, at 8 weeks $n = 3$, at 12 weeks $n = 3$. ($*P < 0.05$ versus control, $^{\#}P < 0.05$ versus injection).

myoblasts.[23] The MDSC's ability to survive within the injured microenvironment and to act as a reservoir of secreting paracrine factors that promote angiogenesis within the injected area, appear to represent possible mechanisms by which these cells repair the heart.[23]

Although MDSCs survive better than conventional myoblasts, it is clear that a large number of the injected cells still suffer from early cell death and other limitation such as poor spreading at the injection site especially when injected in injured myocardium. Also, arrhythmias are a serious safety concern when using cells isolated from skeletal muscle. Therefore, in this study, we sought to evaluate the use of an MDSC sheet as an optimal delivery system to further improve the regenerative capacity of MDSCs in a chronic ischemic heart injury model, and to examine the prevalence of arrhythmias in MDSC injection compared with MDSC sheet implantation. The effect of the sheet delivery system on the ability of MDSCs to improve the contractility of the injured heart, cell survival, angiogenesis, and fibrosis were also determined and compared with conventional intracardiac delivery of MDSCs.

RESULTS

MDSC-seeded sheet characterization

We were able to construct an MDSC sheet with temperature-responsive dishes. The cell sheet spontaneously detached from the surface of the temperature-responsive dishes after a 20–30 minutes incubation at room temperature (Figure 1a). Cross-sectional analysis of the sheet (50–100 μm thick) revealed a higher number of desmin-positive cells, while only a few number of cells were detected when we stained for fsMHC (Figure 1d-f). Lac-Z staining revealed β-galactosidase expression in the MDSC sheets (Figure 1b).

Higher expression of vascular endothelial growth factor was measured in the supernatant used to culture MDSC-seeded sheets

The expression of vascular endothelial growth factor (VEGF) quantified by enzyme-linked immunosorbent assay analysis was also detected in the supernatant of the MDSC-seeded sheets. The estimated concentration of VEGF in the supernatant used to culture the MDSC sheets was significantly higher than what was observed in MDSCs cultured in a monolayer (without sheet). ($P < 0.05$) (Figure 1c).

Echocardiography

Cardiac function was followed for 12 weeks after cell therapy. A constant increase of the end diastolic area was observed in the control group. However, in the MDSC-seeded sheet and MDSC injection group, the end diastolic area was reduced when compared with the control but the difference was only significant between the MDSC-seeded sheet and the control group. This indicates that the prevention of left ventricle (LV) dilation was significantly better in the MDSC-seeded sheet group at 12 weeks post-transplantation, when compared with the other groups (end diastolic area (mm²), S (MDSC sheet): 15.3 ± 0.6; I (MDSC injection): 17.0 ± 1.0; C (control sham): 18.6 ± 1.7, $P < 0.05$, analysis of variance (ANOVA), Figure 2a).

The fractional area change, which represents two-dimensional systolic function, showed an improvement at 8 and 12 weeks post-transplantation in both the MDSC-seeded sheet and the MDSC injection groups when compared with the control group (fractional area change (%) at 8 weeks, S: 35.4 ± 2.5, I: 32.1 ± 3.6, C: 20.3 ± 2.8, $P < 0.05$, ANOVA, Figure 2b). The MDSC-seeded sheet group displayed a better systolic function when compared with the MDSC injection group at 12 weeks (fractional area change (%), S: 37.2 ± 2.0, I: 29.0 ± 3.2, C: 17.8 ± 3.0, $P < 0.05$, ANOVA, Figure 2b). These data suggest that among all groups tested, MDSC-seeded sheet implantation was the most effective treatment for preventing LV dilation and improving systolic function.

Histological analyses of the treated hearts

Scar tissue area was assessed by Masson's trichrome staining. In the MDSC sheet group, an increase in wall thickness was observed

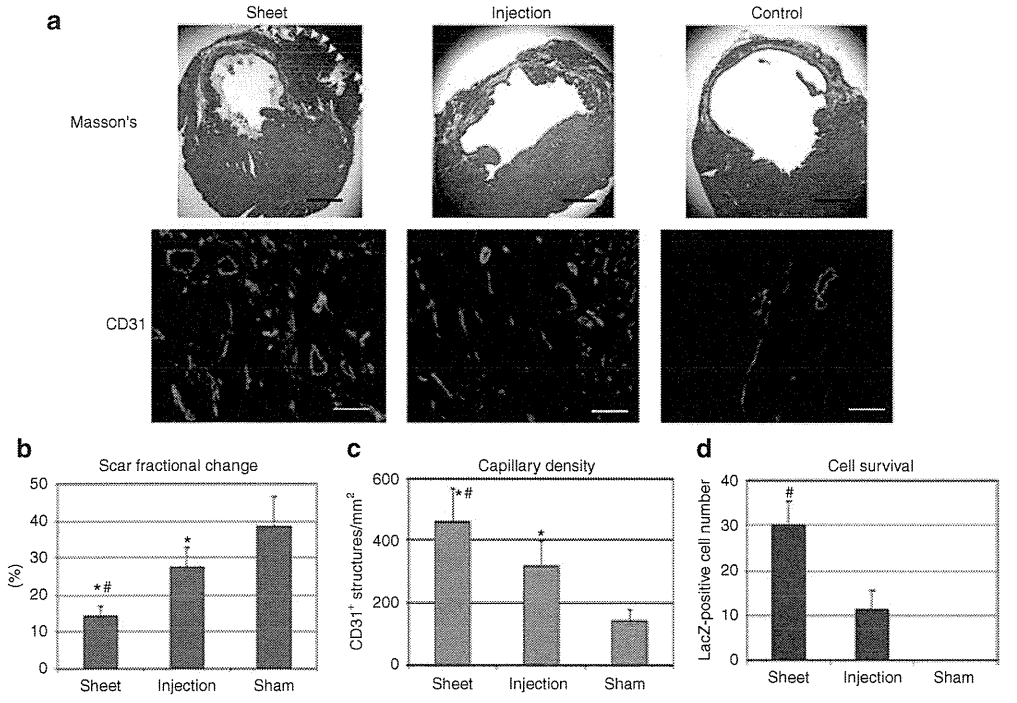

Figure 3 Scar, capillary formation, and cell survival. (**a**) Representative images taken from transverse sections of the left ventricle of each group, stained by Masson's trichrome (muscle is stained red, collagen blue). (Yellow arrow heads, engrafted cell sheet tissue, bar = 1 mm). Immunofluorescence staining of capillary density, as determined by CD31 immunostaining of the infarct regions within sheet, injection, and sham control hearts at 12 weeks after implantation. (Bar = 100 μm). (**b**) Compared with the sham control group, the sheet and injection groups formed a significantly smaller scar tissue areas at 12 weeks after cell transplantation. Sheet group has a significantly lower scar tissue fraction than that of injection group. (**c**) The capillary density of sheet and injection group is significantly higher than control. The sheet group has significantly higher capillary density than injection group. (**d**) We assessed the transplanted cell survival by measuring the number of LacZ-positive cells. The MDSC sheet cells survived in a more effective manner than injected MDSC at 12 weeks after treatment. ($^{*}P < 0.05$ versus control, $^{\#}P < 0.05$ versus injection). MDSC, muscle-derived stem cell.

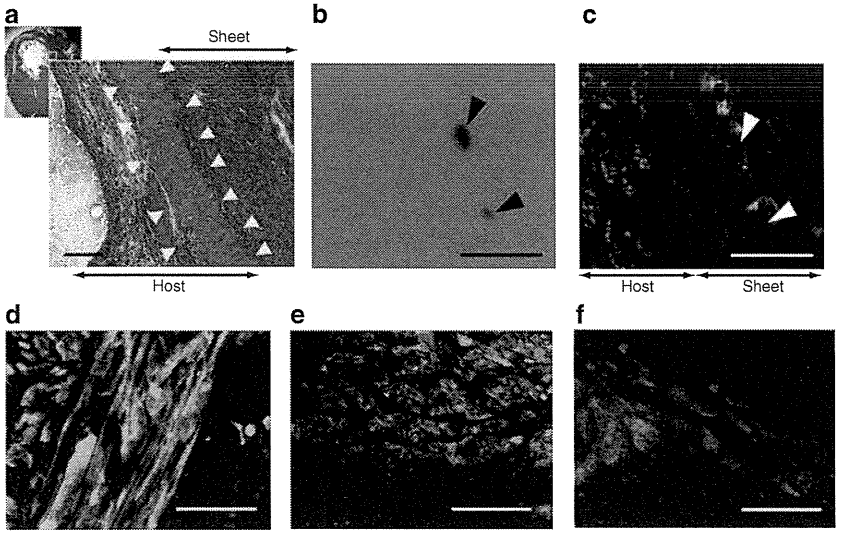

Figure 4 Engraftment of implanted MDSC sheets. (**a**) Masson's trichrome stain at the sheet implantation area at 12 weeks. MDSC sheets attached to the host heart and formed skeletal muscle tissue. The residual cardiomyocytes in the host aligned along the implanted sheet (yellow arrow heads). Bar = 100 μm. (**b**) Engrafted Lac-Z–transduced MDSC cells stained blue in the implanted hearts (black arrow heads). Bar = 50 μm. (**c**) Fast skeletal myosin heavy chain (fsMHC)-positive (green) immunostaining, co-localized with LacZ-positive cells (white arrow heads). In the image, the fsMHC-postive myofibers are stained green, nuclei blue, and cTnI-positive cardiomyocytes are stained red. Bar = 50 μm. (**d–f**) VEGF and fsMHC staining in infarction area at 12 weeks following MDSC implantation. (**d**) VEGF-positive (red) cells are co-localized with fsMHC-positive (green) muscle fibers which formed muscle tissue-like structure along the borderline between sheet and host heart. (**e**) Spotty clustered cells were also stained both with VEGF and fsMHC in the injection group. (**f**) There are some cells stained with VEGF in the infarction area of the control group. Bar = 20 μm. MDSC, muscle-derived stem cell; VEGF, vascular endothelial growth factor.

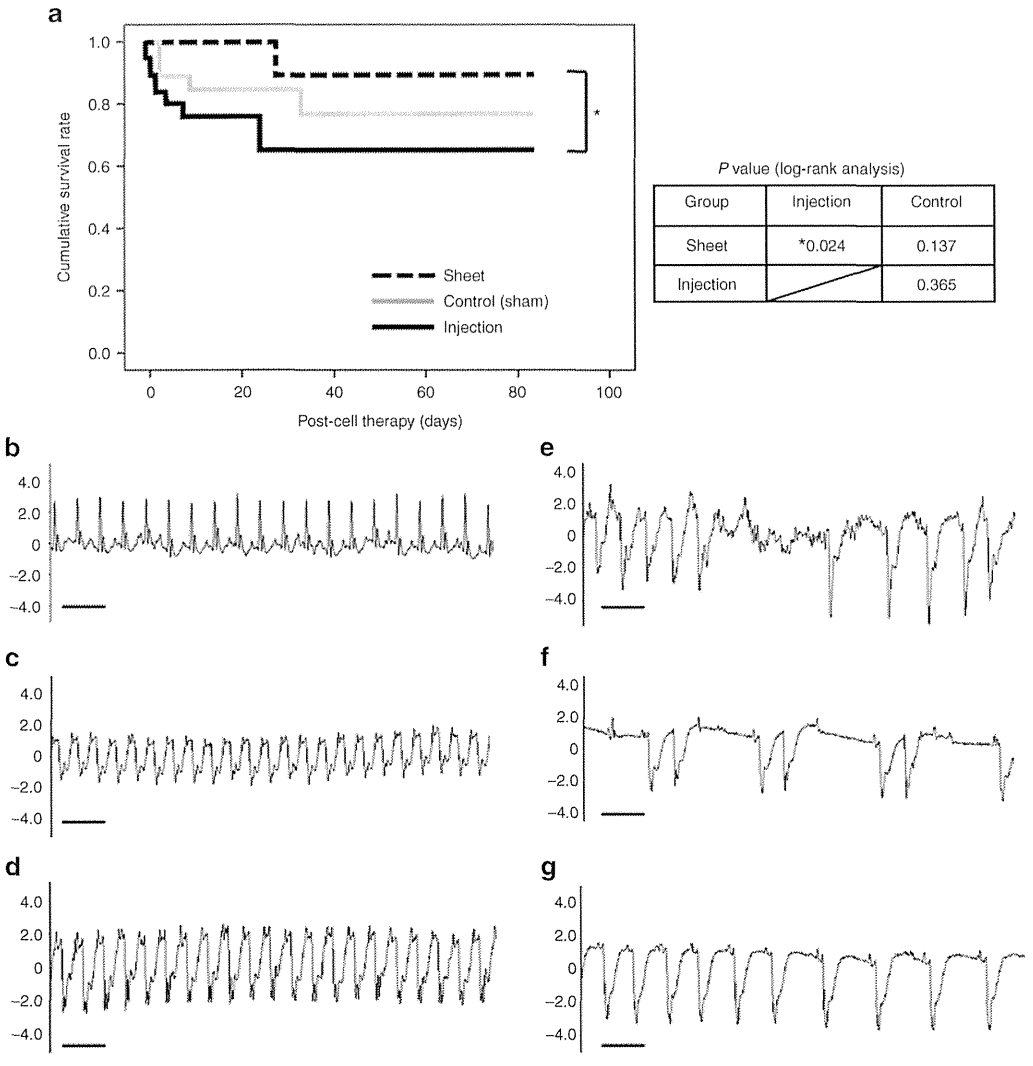

Figure 5 Overall survival rate of mice and representative waveforms of electrocardiogram (ECG). (**a**) Cumulative survival rate 12 weeks after cell therapy in sheet implantation, cell injection, and sham operation groups (n = 19 in each group). (**b**–**g**) Representative ECG of MDSC implanted hearts. Healthy normal ECG ((**b**) 14-week-old healthy male control, (**c**) MDSC sheet group, (**d**) MDSC injection group). Arrhythmic events within 1 week after cell injection ((**e**) irregular beats after transient ventricular tachycardia, (**f**) ventricular bigeminy, (**g**) bradycardia). MDSC, muscle-derived stem cell (x-axis is time period, 0.2 seconds; y-axis is mV).

at 12 weeks postimplantation which was likely a contributing factor in the prevention of the LV dilation observed. Wall thickness was also preserved, at least in part, in the MDSC injection group. However, in the control group, a thin infarction wall and consequently a dilated LV was observed at the same timepoint (Figure 3a). The quantification of scar tissue revealed that the MDSC sheet and MDSC injection groups displayed a reduction in scar tissue formation within the infarct area when compared with the control group (scar fractional change (%), S: 14.3 ± 0.6, I: 27.5 ± 1.2, C: 38.7 ± 1.8, $P < 0.05$, ANOVA, Figure 3b).

In comparison with the control group, the infarcted area in the MDSC sheet and MDSC injection groups contained significantly more CD31-positive cells. The MDSC sheet group has the highest CD31 -positive cell density among all groups tested (capillary density (/mm^2), S: 459.2 ± 20.3, I: 318.9 ± 15.0, C: 142.0 ± 6.7, $P < 0.05$, ANOVA, Figure 3c). We counted the number of LacZ-positive cells to assess cell survival and our results indicated that a greater number of LacZ-expressing cells were observed in the MDSC-seeded sheet group when compared with the MDSC injection group at 12 weeks postimplantation (Lac-Z$^+$ cell number, S: 30.2 ± 5.2, I: 11.2 ± 4.3, C: 0, $P < 0.05$, ANOVA, Figure 3d).

MDSC-seeded sheets form organized (aligned) myotubes and muscle fibers within the transplanted hearts

The MDSC-seeded sheets attached onto the infarcted heart with the migration of a few cells into the native myocardium. Few implanted Lac-Z–positive cells (white arrow, Figure 4c) were co-localized with fsMHC (green) within the MDSCs sheet group. Host cardiac cells, observed just below the graft borderline, stained positively for cardiac troponin-I (red) (Figure 4c). After 12 weeks, residual cardiac muscle cells persisted between the scar tissue area and the MDSC sheet border (yellow arrow, Figure 4a). The MDSCs within the implanted sheet formed a muscle-like

tissue with striated fsMHC-positive myofibers, whereas the direct injection of MDSCs into the myocardium resulted in spotty cell clusters in the host myocardium with an absence of muscle tissue-like formation (green, Figure 4d,e), VEGF expression (red) was detected within the MDSC-seeded sheets and the MDSC injection group at the injection site (red, Figure 4d,e). As expected, VEGF expression was also observed in the native cardiac muscle tissue in the control group (red, Figure 4f).

Arrhythmic events and mice survival after CCM

The cumulative survival rates were analyzed by the Kaplan–Meier method ($n = 19$, in each group, Figure 5a). While the survival rate of the mice in the MDSC sheet and direct MDSC injection groups had no statistical differences compared with the sham infarction group, the MDSC sheet implantation group displayed a significantly higher survival rate than the direct intramyocardial injection group ($P = 0.024$ versus myocardial injection). We also monitored the electrocardiograms of the mice after MDSC transplantation for 12 weeks. To do this, we implanted electrocardiogram telemetry sensors into the mice ($n = 3$ for infarct control, $n = 5$ for the direct injection group and MSDC sheet group). In comparison to the normal healthy controls (Figure 5b), the MDSC post-transplanted animals had deep Q waves 1 week after the MDSC transplantation (MDSC sheet; Figure 5c, MDSC injection; Figure 5d). Although all electrocardiogram-monitored animals survived for 12 weeks after MDSC transplantation, the animals in the direct MDSC injection group (3/5 monitored) had several serious ventricular arrhythmic events including ventricular tachycardia with irregular beats (Figure 5e), bigeminy (Figure 5f), and bradycardia (Figure 5g), which were noted within the first week after the MDSC injection. However, we did not detect these arrhythmic events in the animals in the MDSC sheet implantation group.

DISCUSSION

Skeletal myoblasts have been widely investigated for CCM. In recent clinical studies, lethal ventricular arrhythmias have been noted in the ischemic hearts of patients after direct skeletal myoblast injection.[14] Another cell delivery method, retrograde myoblast delivery from the coronary sinus, was reported to reduce the risk of arrhythmic events.[16] It has also been observed that cell sheets made of skeletal myoblasts appear to eliminate the risk of arrhythmia in the animal models studied.[24] Since we have already shown that direct injection of MDSCs repaired an acute infarction in a more effective manner than myoblasts,[23] the current study aimed to determine whether MDSC sheet technology could further improve the regeneration of the post-infarcted myocardium. The regenerative potential of the MDSCs delivered in sheets or injection forms (direct injection into the myocardium) were compared for their VEGF secretion, angiogenic capabilities, their capacity to inhibit fibrosis, and their ability to improve cardiac function while reducing arrhythmia by electrocardiography.

In vitro, the MDSC sheets secreted more VEGF into the supernatant medium they were cultured in compared with the typical monolayer-cultured MDSCs (Figure 1c). Because these cells were cultured at such a high density, the cells would have experienced relatively hypoxic conditions, which we have shown before to increase the expression of VEGF.[25] *In vitro*, the MDSC sheets had greater expression of desmin than fsMHC. This may be due to the fact that desmin is an earlier myogenic marker than fsMHC and the MDSCs remained less differentiated in the cell sheet group (Figure 1e,f). Besides angiogenesis, MDSC sheet implantation had a direct mechanical protective effect on the thin infarcted ventricular wall.[18,24,26] As in previous studies using cell sheets, the MDSC sheets prevented ventricular dilation more effectively than the direct cell injection group.[26] The prevention of dilation may be due to the physical girdling of the cell sheet which has been shown to prevent remodeling.[26] The cell sheet may help to increase the wall thickness of the infarcted LV and thus decrease ventricular wall stress.[17] Histological analysis revealed that there were more differentiated muscle cells (myotubes and myofibers) that formed muscle tissue-like structures within the implanted MDSC sheets. (Figure 4d). When the MDSC sheets were implanted on the recipient hearts, they would have received direct cyclic mechanical stretching forces from the beating of the heart which led to the organized formation of skeletal muscle fibers across the infarct region verses the disorganized clusters of skeletal muscle cells present in the injection group. Indeed, previous studies have shown that passively stretched myotubes aligned into the direction parallel to the direction of the stretch *in vitro*.[27,28] Furthermore, in a previous study, MDSCs had more VEGF secretion under cyclic mechanical stretch stimulation than under normal conditions.[25] Thus, we hypothesize that the MDSC sheets were influenced both from stretching forces and low oxygenation in the microenvironment of the heart. Consequently, they were more angiogenic and formed more aligned myotubes/myofibers that better protected the heart from dilation when compared with MDSCs that were directly injected into the heart.

In the MDSC injection group, several mice displayed temporary arrhythmic events within 1 week after MDSC transplantation (Figure 5e–g), which was not seen in the MDSC sheet or sham control groups. The risk of arrhythmias may be due to the direct intramyocardial injection of such a large number of cells (2 million cells per mouse heart) since these events were not previously observed by our research groups when smaller number of cells were injected.[23,29] The survival rate of the cells in the MDSC injection group was also significantly lower than the MDSC sheet group (Figure 5a); hence, our results suggest that the arrhythmias observed in the injection group could be caused by the injection of such a large number of cells which might have contributed to poor cell survival and ultimately to the early death (within 1 week) of the mice after MDSC injection. Considering all of our results, we believe that MDSC sheet implantation has many advantages over conventional direct cell injection including the delivery of numerous cells with a better survival capacity that can cover the infarct region with myotubes/myofibers and increase VEGF expression. This increase in VEGF can then promote angiogenesis in the host heart, and ultimately lower the risk of arrhythmias and improve functional outcome; however, it should be noted that although the MDSC sheet group has significantly improved function over the control group, the values do not go all the way back down to normal. The beneficial effect imparted by the cell sheets could also be related to various other factors such as: (i) the fact that cell growth within the sheet exposes the cells to intercellular stretch forces different from those observed from conventional cell culture,[30] which could potentially reduce the cells' adhesion to the hard

surface of the polystyrene culture dishes. In fact, substrate rigidity has been found to have an unfavorable effect on cell proliferation, differentiation, and survival;[31,32] (ii) cell detachment from the culture dish without the need to trypsinize the cells is very beneficial since trypsin can have a negative effect on the cells including the elimination of cell surface molecules, the removal of extracellular matrix, and an overall reduction in the cells viability.

In our study, the fact that the infarcted hearts treated with MDSC sheets had less arrhythmic events compared with those injected directly with the MDSCs, could potentially be attributed to the alignment of the cell sheet myofibers with the host myocardium, which could allow the MDSCs a better reaction in response to the pulsation of the host myocardium; however, the exact mechanism for the reduction in arrhythmic events remains unclear and will require further evaluation in future studies. Further studies would also include ways to optimize the cell sheet therapy in order for the cell sheet to more easily form connection with the cardiac tissue. One way to achieve this is through methods of reducing fibrosis around the implantation area which may serve as a barrier to effective communication between the implanted sheet and the native myocardium.

We have previously demonstrated that sorted human skeletal muscle cells (myoendothelial cells, cells that express both myogenic and endothelial markers) could repair acutely infarcted hearts, and demonstrated better angiogenesis, growth factor expression, and increased cardiac function than more differentiated cell groups tested (endothelial and myogenic cells).[29] Thus, in the future, we will apply the cell sheet technique to this promising human cell source in order to bring this beneficial technology closer to translational studies for ischemic heart failure patients.

In conclusion, MDSC sheet implantation could represent a promising delivery method for CCM for the treatment of patients with chronic cardiac ischemia. This method was shown to improve cardiac repair and function after MDSC sheet implantation and decrease the incidence of arrhythmias, which could represent an important cell delivery approach to improve the success of CCM utilizing both murine and human muscle-derived progenitor cells.

MATERIALS AND METHODS

MDSC preparation and retroviral transduction. MDSCs were isolated *via* the modified preplate technique[21,22,33] and were cultured in proliferation medium, which contains Dulbecco's modified Eagle's medium(GIBCO-BRL, Grand Island, NY), 10% fetal bovine serum (GIBCO-BRL), 10% horse serum (GIBCO-BRL), 1% penicillin/streptomycin (GIBCO-BRL), and 0.5% chick embryo extract (Accurate Chemical, Westbury, NY).[21] The isolated MDSCs were plated in collagen-coated 25 cm^2 flasks at a density of 3×10^5 cells per well in proliferation medium. At 70% confluence, the cells were dissociated with trypsin/EDTA (GIBCO-BRL), replated at a cell density of $1.0–2.5 \times 10^3$ cells/cm^2 and cultured for 3–4 weeks before performing the cell treatment described below. To track donor cell fate after injection, the MDSCs were transduced with a retrovirus encoding for a nuclear-localized LacZ (nLacZ) reporter gene as previously described.[25,34]

Cell sheet construction. LacZ-transduced MDSCs were incubated in 175 cm^2 flasks at a density of 3.0×10^5 cells in each flask. When the cells became ~70% confluent, they were dissociated from the flasks with trypsin–EDTA and re-incubated on 12-well temperature-responsive culture dishes (UpCell; NUNC, Rochester, NY) at 37 °C, with the cell number adjusted to 2.0×10^6 per well. The culture dishes are coated with a temperature-responsive polymer (poly(N-isopropylacrylamide)). This substance is hydrophobic at 37 °C and then becomes hydrophilic at room temperature which allows the cell layer to be released from the dish without trypsin.[26] After 17 hours, the dishes were incubated at room temperature for 20 minutes. During that time, the cell sheet detached spontaneously to generate free-floating, monolayer cell sheets. Each sheet was stained for desmin, fsMHC, and X-gal (blue) as shown in Figure 1a,b.

VEGF expression in the supernatant. We estimated the expression of VEGF in the supernatant of the MDSC sheet and compared the results with MDSCs *in vitro*. The MDSC sheets (which contains 2 million MDSCs) were incubated in collagen-coated 6-well dishes for 24 hours. The same number of MDSCs was also cultured in similar size dishes for 24 hours. We then measured the amount of VEGF that was secreted into the supernatant by an enzyme-linked immunosorbent assay (R&D Systems, Minneapolis, MN), as previously described.[25]

Animal surgery. The Institutional Animal Care and Use Committee, University of Pittsburgh, approved the animal and surgical procedures performed in this study (protocol 0903420-1). A total of 60 male non-obese diabetic severe combined immunodeficiency mice (The Jackson Laboratory, Bar Harbor, ME) were used for this study.

A chronic infarction model was used to assess the cardiac transplantation efficacy of injection versus cell sheet delivery of MDSCs. Mice were randomly allocated between the treatment groups (MDSCs-seeded sheet, MDSCs injection, phosphate-buffered saline injection) and all mice underwent permanent left anterior descending coronary artery ligation to create a myocardial infarct. Two weeks later, the chest cavity was re-opened and treatment was performed. In the MDSC sheet group, a constructed MDSC-seeded sheet was made by seeding 2.0×10^6 cells per well in a 12-well plate (UpCell) and applied to the surface of the heart to cover the infarcted scar area as previously described.[26] In the MDSC injection group, 2.0×10^6 cells in a solution of 30 µl of phosphate-buffered saline per heart were injected into the hearts of mice 2 weeks after inducing the myocardial infarction as previously described.[23] In the control group, a sham operation was performed.

Echocardiography. Echocardiography was performed by a blinded investigator to assess the heart function, as previously described.[23] The cardiac function was analyzed at baseline (2 weeks after infarction), 4, 8, and 12 weeks after cell therapy. LV infarction size was estimated using a standard short-axis view by the percentage of scar area to LV free wall area. All mice used in the study were selected with >25% infarction.[35]

Histology. Mice were sacrificed and their hearts harvested, flash-frozen in 2-methylbutane pre-cooled in liquid nitrogen, and serially cryosectioned from the apex to the base of each heart into sections 5–10 µm thick. Previously described techniques were used to stain the sections for both nLacZ and eosin.[21] Staining for cardiac- and skeletal-specific markers, donor-derived cell markers, CD31 and VEGF were performed according to the following protocols. Cryosections were fixed in 2% formaldehyde then stained for nLacZ expression in X-Gal solution overnight at 37 °C. For the VEGF, cTn1/fsMHC staining, rabbit anti-VEGF (Abcam, Cambridge, MA) was incubated overnight at a 1:200 dilution followed by donkey anti-rabbit Alexa Fluor 594 (Molecular Probes, Grand Island, NY). Next, goat anti-cTn1 was incubated for 2 hours at a 1:20,000 dilution followed by incubation with donkey anti-goat Alexa Fluor 555 (Molecular Probes). Subsequently, the slides were blocked using the mouse-on-mouse kit (M.O.M. kit; Vector Labs, Burlingame, CA) according to the manufacturer's protocol. Following the MOM blocking step, the sections were incubated in mouse anti-fast skeletal myosin (MY-32) diluted to 1:400 for 30 minutes followed by donkey

anti-mouse IgG Alexa Fluor 488 at 1:400. For the CD31 staining, sections were fixed in 4% formalin followed by blocking with 10% donkey serum. The primary antibody was rat anti-mouse CD31 (1:100) followed by anti-rat Alexa Fluor 555 (1:200). Nuclei were revealed with 4′,6-diamidino-2-phenylindole (DAPI) stain (100 ng/ml; Sigma-Aldrich, St Louis, MO). All fluorescence and bright-field microscopy was performed using either a Nikon Eclipes E800 with a Retiga EXi digital camera (Q Imaging, Burnaby, British Columbia, Canada) or a Leica DMIRB microscope equipped with a Retiga 1300 digital camera (Q Imaging). Images were acquired with Northern Eclipse software (v6.0; Empix Imaging, Cheektowaga, NY).

Estimate of nLacZ+ cells in hearts after cell therapy. nLacZ+ cells were counted within serial sections (10 μm in thickness) cut from the apex to the base of the injected hearts. Because the serial sections were obtained every 100 μm (10 sections per sample), an estimate of the total number of nLacZ+ cells counted in all serial sections was multiplied by a factor of 10, using a protocol previously described.[36]

Capillary density. The CD31+ vessels in the entire infarcted area were counted in hearts implanted with the MDSC sheets, injected with MDSCs and sham controls (at 12 weeks after therapy, $n = 5$ in each group) by a blinded investigator. Capillary density was expressed as the number of CD31+ structures per square millimeter, as previously described.[37]

Scar tissue formation. We used a Masson's trichrome staining kit (IMEB, San Marcos, CA) to stain collagen deposition on cryosections of the heart. The scar tissue area and the area of the entire cardiac muscle sections were measured using digital image analyzer software (Image J; National Institutes of Health, Bethesda, MD). The scar area fraction was calculated as the ratio of scar tissue area to the entire cardiac muscle area and was averaged from seven sections per heart.

Arrhythmia assessment. Spontaneous arrhythmia occurrence was assessed by telemetry (Data Sciences International, New Brighton, MN).[38,39] A transmitter with two electrodes was implanted subcutaneously on the back of the mice after treatment and monitored for 24 hours 1, 3, 7 days, and 2, 4, 8, and 12 weeks after therapy ($n = 3$, each group). The recorded electrocardiography waveforms were retrieved and calculated using DSI software (DSI Dataquest A.R.T. Analysis; Data Science International).

Statistical analysis. All measured data are presented as the mean ± SE. A Kaplan–Meier survival curve estimation with log-rank test was performed to compare the survival rate among experimental groups. For the analysis of the echocardiographic data, we applied the two-way repeated ANOVA test and the Tukey's multiple comparison test. The one-way ANOVA and the Tukey's post-hoc tests were performed to analyze the scar formation, capillary density, and cell survival data in all groups. Statistical significance was set at a value of $P < 0.05$. All statistical tests were performed using SPSS Statistics 17.0 (IBM SPSS, Armonk, NY).

ACKNOWLEDGMENTS

We thank Michelle Witt and Jessica Tebbets for their excellent technical assistance and protocol submission to University of Pittsburgh's Institutional Animal Care and Use Committee. We also thank James Cummins for his editorial assistance in the preparation of this manuscript. This work was funded in part by the National Institutes of Health (NIH U54 AR050733 and NIH R21 HL0944402), the Department of Defense (W81XWH-05-1-0334), the Henry J. Mankin Endowed Chair at the University of Pittsburgh, and the William F. and Jean W. Donaldson Endowed Chair at the Children's Hospital of Pittsburgh. J.H. discloses the fact that he received consulting income and royalties from Cook MyoSite, Inc. during the performance period of this project. The other authors declared no conflict of interest.

REFERENCES

1. Tamaki, T, Akatsuka, A, Okada, Y, Uchiyama, Y, Tono, K, Wada, M *et al.* (2008). Cardiomyocyte formation by skeletal muscle-derived multi-myogenic stem cells after transplantation into infarcted myocardium. *PLoS ONE* **3**: e1789.
2. Kessler, PD and Byrne, BJ (1999). Myoblast cell grafting into heart muscle: cellular biology and potential applications. *Annu Rev Physiol* **61**: 219–242.
3. Klug, MG, Soonpaa, MH, Koh, GY and Field, LJ (1996). Genetically selected cardiomyocytes from differentiating embryonic stem cells form stable intracardiac grafts. *J Clin Invest* **98**: 216–224.
4. Min, JY, Yang, Y, Converso, KL, Liu, L, Huang, Q, Morgan, JP *et al.* (2002). Transplantation of embryonic stem cells improves cardiac function in postinfarcted rats. *J Appl Physiol* **92**: 288–296.
5. Toma, C, Pittenger, MF, Cahill, KS, Byrne, BJ and Kessler, PD (2002). Human mesenchymal stem cells differentiate to a cardiomyocyte phenotype in the adult murine heart. *Circulation* **105**: 93–98.
6. Wang, JS, Shum-Tim, D, Galipeau, J, Chedrawy, E, Eliopoulos, N and Chiu, RC (2000). Marrow stromal cells for cellular cardiomyoplasty: feasibility and potential clinical advantages. *J Thorac Cardiovasc Surg* **120**: 999–1005.
7. Gnecchi, M, He, H, Liang, OD, Melo, LG, Morello, F, Mu, H *et al.* (2005). Paracrine action accounts for marked protection of ischemic heart by Akt-modified mesenchymal stem cells. *Nat Med* **11**: 367–368.
8. Hirschi, KK and Goodell, MA (2002). Hematopoietic, vascular and cardiac fates of bone marrow-derived stem cells. *Gene Ther* **9**: 648–652.
9. Orlic, D, Kajstura, J, Chimenti, S, Limana, F, Jakoniuk, I, Quaini, F *et al.* (2001). Mobilized bone marrow cells repair the infarcted heart, improving function and survival. *Proc Natl Acad Sci USA* **98**: 10344–10349.
10. Kocher, AA, Schuster, MD, Szabolcs, MJ, Takuma, S, Burkhoff, D, Wang, J *et al.* (2001). Neovascularization of ischemic myocardium by human bone-marrow-derived angioblasts prevents cardiomyocyte apoptosis, reduces remodeling and improves cardiac function. *Nat Med* **7**: 430–436.
11. Asahara, T, Murohara, T, Sullivan, A, Silver, M, van der Zee, R, Li, T *et al.* (1997). Isolation of putative progenitor endothelial cells for angiogenesis. *Science* **275**: 964–967.
12. Beltrami, AP, Barlucchi, L, Torella, D, Baker, M, Limana, F, Chimenti, S *et al.* (2003). Adult cardiac stem cells are multipotent and support myocardial regeneration. *Cell* **114**: 763–776.
13. Oh, H, Bradfute, SB, Gallardo, TD, Nakamura, T, Gaussin, V, Mishina, Y *et al.* (2003). Cardiac progenitor cells from adult myocardium: homing, differentiation, and fusion after infarction. *Proc Natl Acad Sci USA* **100**: 12313–12318.
14. Menasché, P, Alfieri, O, Janssens, S, McKenna, W, Reichenspurner, H, Trinquart, L *et al.* (2008). The Myoblast Autologous Grafting in Ischemic Cardiomyopathy (MAGIC) trial: first randomized placebo-controlled study of myoblast transplantation. *Circulation* **117**: 1189–1200.
15. Menasché, P (2009). Stem cell therapy for heart failure: are arrhythmias a real safety concern? *Circulation* **119**: 2735–2740.
16. Fukushima, S, Coppen, SR, Lee, J, Yamahara, K, Felkin, LE, Terracciano, CM *et al.* (2008). Choice of cell-delivery route for skeletal myoblast transplantation for treating post-infarction chronic heart failure in rat. *PLoS ONE* **3**: e3071.
17. Zhou, Q, Zhou, JY, Zheng, Z, Zhang, H and Hu, SS (2010). A novel vascularized patch enhances cell survival and modifies ventricular remodeling in a rat myocardial infarction model. *J Thorac Cardiovasc Surg* **140**: 1388–96.e1.
18. Memon, IA, Sawa, Y, Fukushima, N, Matsumiya, G, Miyagawa, S, Taketani, S *et al.* (2005). Repair of impaired myocardium by means of implantation of engineered autologous myoblast sheets. *J Thorac Cardiovasc Surg* **130**: 1333–1341.
19. Kondoh, H, Sawa, Y, Miyagawa, S, Sakakida-Kitagawa, S, Memon, IA, Kawaguchi, N *et al.* (2006). Longer preservation of cardiac performance by sheet-shaped myoblast implantation in dilated cardiomyopathic hamsters. *Cardiovasc Res* **69**: 466–475.
20. Gharaibeh, B, Lu, A, Tebbets, J, Zheng, B, Feduska, J, Crisan, M *et al.* (2008). Isolation of a slowly adhering cell fraction containing stem cells from murine skeletal muscle by the preplate technique. *Nat Protoc* **3**: 1501–1509.
21. Qu-Petersen, Z, Deasy, B, Jankowski, R, Ikezawa, M, Cummins, J, Pruchnic, R *et al.* (2002). Identification of a novel population of muscle stem cells in mice: potential for muscle regeneration. *J Cell Biol* **157**: 851–864.
22. Lee, JY, Qu-Petersen, Z, Cao, B, Kimura, S, Jankowski, R, Cummins, J *et al.* (2000). Clonal isolation of muscle-derived cells capable of enhancing muscle regeneration and bone healing. *J Cell Biol* **150**: 1085–1100.
23. Oshima, H, Payne, TR, Urish, KL, Sakai, T, Ling, Y, Gharaibeh, B *et al.* (2005). Differential myocardial infarct repair with muscle stem cells compared to myoblasts. *Mol Ther* **12**: 1130–1141.
24. Miyagawa, S, Sawa, Y, Sakakida, S, Taketani, S, Kondoh, H, Memon, IA *et al.* (2005). Tissue cardiomyoplasty using bioengineered contractile cardiomyocyte sheets to repair damaged myocardium: their integration with recipient myocardium. *Transplantation* **80**: 1586–1595.
25. Payne, TR, Oshima, H, Okada, M, Momoi, N, Tobita, K, Keller, BB *et al.* (2007). A relationship between vascular endothelial growth factor, angiogenesis, and cardiac repair after muscle stem cell transplantation into ischemic hearts. *J Am Coll Cardiol* **50**: 1677–1684.
26. Sekiya, N, Matsumiya, G, Miyagawa, S, Saito, A, Shimizu, T, Okano, T *et al.* (2009). Layered implantation of myoblast sheets attenuates adverse cardiac remodeling of the infarcted heart. *J Thorac Cardiovasc Surg* **138**: 985–993.
27. De Deyne, PG (2000). Formation of sarcomeres in developing myotubes: role of mechanical stretch and contractile activation. *Am J Physiol, Cell Physiol* **279**: C1801–C1811.
28. Kemp, TJ, Sadusky, TJ, Simon, M, Brown, R, Eastwood, M, Sassoon, DA *et al.* (2001). Identification of a novel stretch-responsive skeletal muscle gene (Smpx). *Genomics* **72**: 260–271.
29. Okada, M, Payne, TR, Zheng, B, Oshima, H, Momoi, N, Tobita, K *et al.* (2008). Myogenic endothelial cells purified from human skeletal muscle improve cardiac

function after transplantation into infarcted myocardium. *J Am Coll Cardiol* **52**: 1869–1880.
30. Miquelard-Garnier, G, Zimberlin, JA, Sikora, CB, Wadsworth, P and Crosby, A (2010). Polymer microlenses for quantifying cell sheet mechanics. *Soft Matter* **6**: 398–403.
31. Engler, AJ, Sen, S, Sweeney, HL and Discher, DE (2006). Matrix elasticity directs stem cell lineage specification. *Cell* **126**: 677–689.
32. Gilbert, PM, Havenstrite, KL, Magnusson, KE, Sacco, A, Leonardi, NA, Kraft, P *et al.* (2010). Substrate elasticity regulates skeletal muscle stem cell self-renewal in culture. *Science* **329**: 1078–1081.
33. Qu, Z, Balkir, L, van Deutekom, JC, Robbins, PD, Pruchnic, R and Huard, J (1998). Development of approaches to improve cell survival in myoblast transfer therapy. *J Cell Biol* **142**: 1257–1267.
34. Zheng, B, Cao, B, Crisan, M, Sun, B, Li, G, Logar, A *et al.* (2007). Prospective identification of myogenic endothelial cells in human skeletal muscle. *Nat Biotechnol* **25**: 1025–1034.
35. Fujimoto, KL, Clause, KC, Liu, LJ, Tinney, JP, Verma, S, Wagner, WR *et al.* (2011). Engineered fetal cardiac graft preserves its cardiomyocyte proliferation within postinfarcted myocardium and sustains cardiac function. *Tissue Eng Part A* **17**: 585–596.
36. Balsam, LB, Wagers, AJ, Christensen, JL, Kofidis, T, Weissman, IL and Robbins, RC (2004). Haematopoietic stem cells adopt mature haematopoietic fates in ischaemic myocardium. *Nature* **428**: 668–673.
37. Kawata, H, Yoshida, K, Kawamoto, A, Kurioka, H, Takase, E, Sasaki, Y *et al.* (2001). Ischemic preconditioning upregulates vascular endothelial growth factor mRNA expression and neovascularization via nuclear translocation of protein kinase C epsilon in the rat ischemic myocardium. *Circ Res* **88**: 696–704.
38. Fernandes, S, Amirault, JC, Lande, G, Nguyen, JM, Forest, V, Bignolais, O *et al.* (2006). Autologous myoblast transplantation after myocardial infarction increases the inducibility of ventricular arrhythmias. *Cardiovasc Res* **69**: 348–358.
39. Howarth, FC, Jacobson, M, Shafiullah, M and Adeghate, E (2006). Effects of insulin treatment on heart rhythm, body temperature and physical activity in streptozotocin-induced diabetic rat. *Clin Exp Pharmacol Physiol* **33**: 327–331.

Biomaterials 34 (2013) 662–668

Contents lists available at SciVerse ScienceDirect

Biomaterials

journal homepage: www.elsevier.com/locate/biomaterials

Network formation through active migration of human vascular endothelial cells in a multilayered skeletal myoblast sheet

Eiji Nagamori [a], Trung Xuan Ngo [b], Yasunori Takezawa [b], Atsuhiro Saito [c], Yoshiki Sawa [c], Tatsuya Shimizu [d], Teruo Okano [d], Masahito Taya [b], Masahiro Kino-oka [a,*]

[a] Department of Biotechnology, Graduate School of Engineering, Osaka University, 2-1 Yamada-oka, Suita, Osaka 565-0871, Japan
[b] Division of Chemical Engineering, Graduate School of Engineering Science, Osaka University, 1-3 Machikaneyama-cho, Toyonaka, Osaka 560-8531, Japan
[c] Department of Surgery, Division of Cardiovascular Surgery, Graduate School of Medicine, Osaka University, 2-15 Yamada-oka, Suita, Osaka 565-0871, Japan
[d] Institute of Advanced Biomedical Engineering and Science, Tokyo Women's Medical University, 8-1 Kawada-cho, Shinjuku-ku, Tokyo 162-8666, Japan

ARTICLE INFO

Article history:
Received 10 August 2012
Accepted 23 August 2012
Available online 30 October 2012

Keywords:
Cell sheet
Vascular endothelial cells
Skeletal myoblasts
Angiogenesis
Cell migration
Image processing

ABSTRACT

Autologous transplantation of myoblast sheet has attracted attention as a new technique for curing myocardial infarction. Myoblast sheet has the ability to secret cytokines that improve heart function via the facilitation of angiogenesis on affected part. To mimic the *in vivo* angiogenesis in the myoblast sheet after transplantation, a five-layered cell sheet of human skeletal muscle myoblasts (HSMMs) was overlaid on human umbilical vein endothelial cells (HUVECs) which enables evaluation of dynamic HUVEC behavior. HUVECs existing initially at the bottom of the sheet changed to be a stretched shape and migrated upward compared with the surrounding HSMMs in the sheet. Prolonged incubation resulted in network formation of HUVECs in the middle of the sheet, although non-networked HUVECs continued to migrate to the top of the sheet, which meant the spatial habitation of HUVECs in the cell sheet. Image processing was performed to determine the variation in the extent of network formation at different HUVEC densities. It was found that the extent of formed network depended on the frequency of encounters among HUVECs in the middle of the sheet. The present system, which can evaluate network formation, is considered to be a promising *in vitro* angiogenesis model.

1. Introduction

Cell sheet engineering has been proposed to be a promising technique to form plate-shaped aggregates, which are thought to mimic tissues available for transplantation [1]. A temperature-responsive poly-(*N*-isopropylacrylamide) (PNIPAAm)-grafted surface can be used to harvest a cell sheet without enzymatic digestion of the intact extracellular matrix on the detached surface [2] to enable the construction of three-dimensional (3-D) multi-layered tissues without scaffolds [3].

Recently, autologous transplantation of myoblast sheet has attracted attention as a new technique for curing myocardial infarction, which is associated with cardiomyocyte dysfunction and irreversible cell loss [4,5]. Skeletal myoblasts, which are relatively easy to harvest from patients, can undergo self-renewal and differentiation, allowing cardio muscle regeneration upon injury. Myoblast sheet also has the ability to secret cytokines that improve heart function via the facilitation of angiogenesis and attraction of progenitors on affected part. The sheet transplantation method can overcome disadvantages of the myoblast injection method, such as loss of transplanted cells due to poor survival of cells [6] and arrhythmic heart beat due to a global down-regulation of connexin 43 in the host heart [7]. Sawa et al. conducted the first clinical trial of the transplantation using myoblast sheet that enables the effective delivery of a sheet for a large coverage area to provide the improvement of damaged heart function *in vivo* without arrhythmic heart beats [8]. Further development of transplantation using the multilayered myoblast sheets showed the improved heart function when compared with monolayer sheet transplantation [9].

From a manufacturing point of view, process and quality controls are important for realizing commercialization of cell sheet transplant. Many studies have addressed cell sources, culture, sheet assembling, and *in vivo* animal tests; however, the method for quality control of myoblast sheets, especially for transplant efficacy such as angiogenesis capability, has not been systematized. Although animal tests can be used to estimate the overall efficacy of the transplants, such methods provide an insufficient estimation

* Corresponding author. Tel.: +81 (0) 6 6879 7444; fax: +81 (0) 6 6879 4246.
E-mail address: kino-oka@bio.eng.osaka-u.ac.jp (M. Kino-oka).

0142-9612/$ – see front matter © 2012 Elsevier Ltd. All rights reserved.
http://dx.doi.org/10.1016/j.biomaterials.2012.08.055

of product quality for autologous transplantation because of the lack of quantitative analysis and non-human estimation as well as patient dependence. Thus, it is necessary to create a method that is suitable for *in vitro* quantitative estimation of the transplants.

In a previous study, a five-layered human skeletal muscle myoblast (HSMM) sheet was constructed to determine sheet fluidity by confocal laser scanning microscopy with image processing [10]. In the present study, an *in vitro* system based on a multilayered HSMM sheet with human umbilical vein endothelial cells (HUVECs) was developed to mimic the *in vivo* angiogenesis in the HSMM sheet after transplantation. Image processing was performed to evaluate the HUVEC spatial distribution and network formation in the HSMM sheet to elucidate the spatial habitation arising from HUVEC migration and connection.

2. Materials and methods

2.1. Cell preparation

HSMMs (Lot. No. 4F1618; Lonza Walkersville Inc., Walkersville, MD) and HUVECs (Lot. No. 4F0709; Lonza Walkersville Inc.) were used in the experiments. According to procedures described elsewhere [11], subcultures of HSMMs on laminin-coated surfaces were conducted at 37 °C in an atmosphere of 5% CO_2 in Dulbecco's Modified Eagle's Medium (DMEM; Sigma–Aldrich, St. Louis, MO) containing 10% fetal bovine serum (FBS; Invitrogen, Grand Island, NY) and antibiotics (100 U/cm^3 penicillin G, 0.1 mg/cm^3 streptomycin, and 0.25 mg/cm^3 amphotericin B; Invitrogen). HUVECs were cultured in a commercially available medium (EGM-2; Lonza Walkersville Inc.). The medium depth was set to 2 mm throughout the experiments.

2.2. Incubation of five-layered HSMM sheet with HUVECs

Five-layered HSMM sheet was fabricated according to a previously reported method [10]. In brief, as shown in Fig. 1A, starter HSMMs prepared by subculturing were stained with CellTracker™ Orange (Invitrogen) to obtain fluorescent orange cells according to a commercially recommended protocol (5 μM for 15 min for live cell imaging). The HSMMs were seeded at 2.3 × 10^5 cells/cm^2 in each well (1.9 cm^2) of 24-well UpCell™ plates (CellSeed, Tokyo, Japan) with a temperature-responsive surface grafted with PNIPAAm and incubated for 24 h at 37 °C in a 5% CO_2 atmosphere to form the monolayer sheet. To stack monolayer sheets to fabricate the multilayered cell sheet, the customized stamps with the gelatin gel (G1890-100G; Sigma–Aldrich) were used. To harvest the monolayer sheet, the stamp with the gelatin gel was overlaid on the monolayer sheet in a well at 37 °C, and the temperature was shifted to 20 °C. After 30 min, the stamp was lifted together with the monolayer sheet from the bottom surface of the well. The steps were then repeated for the sequential harvests of monolayer sheets to form the multilayered construct on the stamp. The multilayered sheet with the gelatin was peeled from the stamp for transfer to a dish containing the precultured HUVECs. For the preculture, HUVECs were seeded into culture dishes (35 mm in diameter; Corning Inc., NY) and cultured in the EGM-2 medium for 24 h. The initial density of HUVECs (X_0) for the subsequent incubation with the sheet was set in the range of 0.35–3.32 × 10^4 cells/cm^2 by changing the seeding density of HUVECs (X_s). The relationship between X_s and X_0 was determined in advance (Supplementary Table 1). After incubation at 20 °C for 2 h, the sheet was incubated at 37 °C in DMEM containing 10% FBS for 1 h to remove the gelatin. The medium containing the dissolved gelatin was exchanged with fresh medium. At the given incubation time (t), triplicate samplings were performed for quantitative analysis. During the incubation period, the medium was renewed every day.

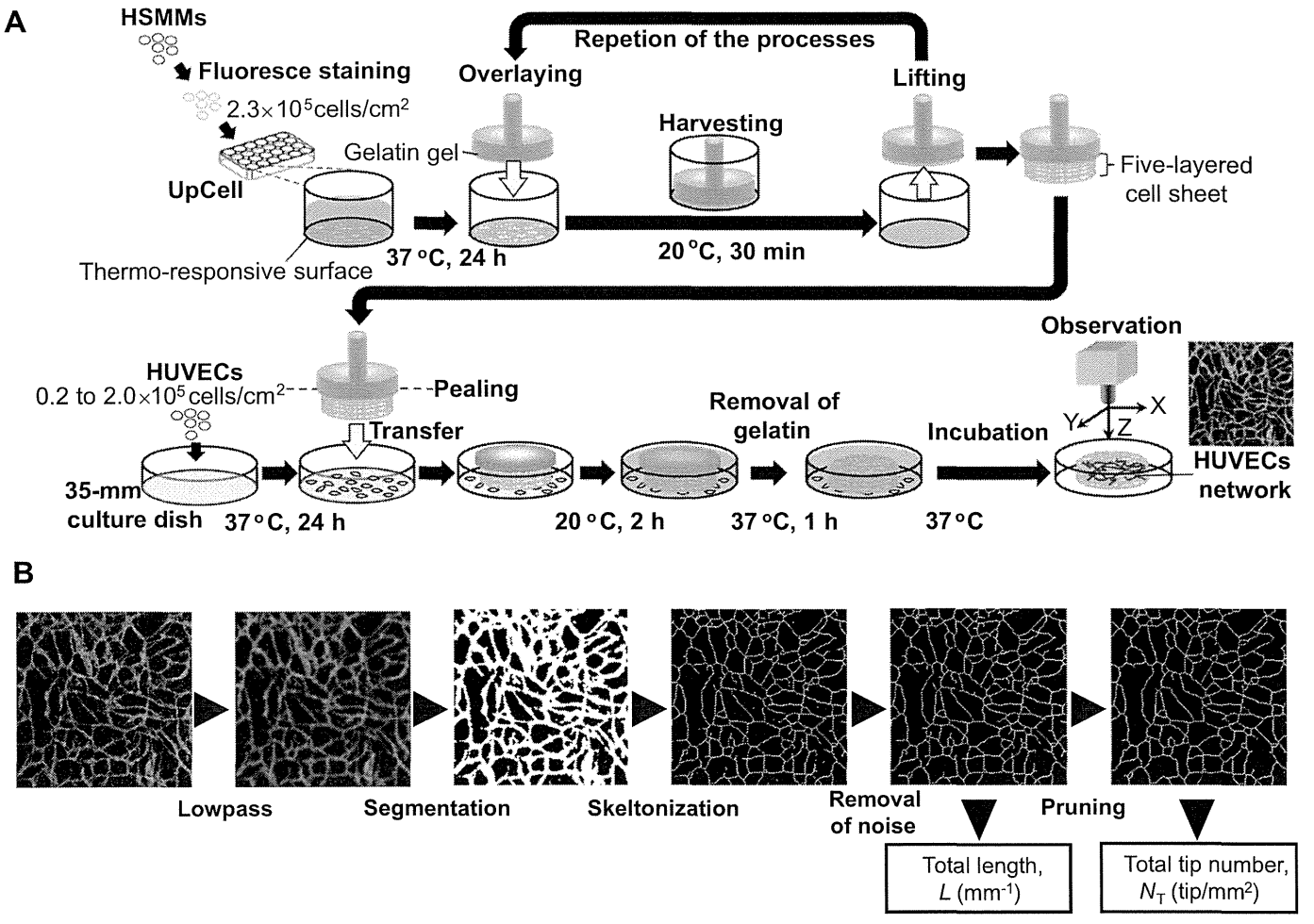

Fig. 1. Schematic drawings of experimental procedures. A: Construction of multilayered HSMM sheet and incubation with HUVECs. B: Image process procedure to evaluate HUVEC network formation and maturation.

2.3. Immunostaining for HUVECs

The culture system containing the five-layered HSMM sheet with HUVECs was washed with phosphate-buffered saline (PBS) and fixed in PBS containing 4% paraformaldehyde (Wako Pure Chemical Industries, Osaka, Japan) overnight. The fixed specimen was then permeabilized in PBS containing 0.1% Triton X-100 (Wako Pure Chemical Industries) for 12 min, washed twice with PBS, and then blocked in 1% bovine serum albumin (BSA; Wako Pure Chemical Industries) in PBS for 1 h. The specimen was labeled with a primary antibody (monoclonal mouse anti-human CD31 antibody; DAKO, Glostrup, Denmark) in 1% BSA solution overnight. The specimen was then thoroughly washed with PBS and immersed in 1% BSA solution containing the secondary antibody conjugated with Alexa Fluor® 488 (Invitrogen) for 1 h.

2.4. Evaluation of the HUVEC network formed inside the HSMM sheet

The image capture was carried out using a 10× objective lens of confocal laser scanning microscope (FV-300; Olympus, Tokyo, Japan) at more than 8 positions in each sample. As shown in Fig. 1B, each image was 8-bit gray scale with a size of 256 × 256 pixels and covered an area of 942 × 942 μm. The images were subjected to image processing (Image-Pro Plus; Media Cybernetics Inc., Bethesda, MD) using a low-pass filter for primary noise removal and binarization with a certain intensity threshold. The threshold intensity was determined as the average of the mode intensity and the automatic threshold intensity calculated with an Otsu adaptive threshold algorithm [12], which chooses the threshold to minimize the intra-class variance of the thresholded black and white pixels with an exhaustive search. The binary images were subjected to skeletonization to produce lined objects, the secondary noise removal with a size threshold to remove items with a size of less than 16 pixels, and the pruning of small branches in the objects. The total length of the network per image area (L; cm^{-1}), and the number of total tips of the network (N_T; tip/cm^2), were measured to estimate the extent of the HUVEC network (L/N_T; cm/tip). The tips existing at the edge of the image were not counted.

2.5. Spatial distribution of HUVECs and HSMMs in five-layered HSMM sheets

To determine the vertical distribution of the HUVECs inside the HSMM sheet, the green cells (HUVECs labeled with Alexa Fluor 488) and orange cells (HSMMs stained with CellTracker™ Orange) in each layer were observed and quantitatively analyzed as previously described [10] (Supplementary Fig. 1). The number of colored pixels in each slice was counted. The green and orange pixels in each slice were normalized using the maximum green and orange pixel values, respectively, found in all of the slice images. Slices possessing more than 10% of the colored pixels were regarded to exist inside the cell sheet, from which the vertical positions at the top and bottom of the five-layered sheet, and the sheet thickness, h (μm), were determined. The green pixels inside the sheet were normalized to determine the vertical distribution of the green pixels by dividing them into 5 layers. The normalized distribution of the green pixels was assumed to be equivalent to the distribution of green cells in the sheet, which was determined as the frequency of green cells, f_G (−), in each layer. For determination of the vertical distribution of the HSMMs, HSMMs stained with CellTracker™ Green (Invitrogen) were placed in the bottom layer of a five-layered HSMM sheet, and their vertical distribution at 24 h was determined.

3. Results

3.1. HUVEC network formation inside the HSMM sheet

The behavior of HUVECs in the five-layered HSMM sheet was observed for 120 h to estimate the growth and network formation according to the parameters L, N_T, and L/N_T. The initial density of HUVECs was set at $X_0 = 1.29 \times 10^4$ cells/cm^2. At the beginning of the incubation period ($t = 0$), as shown in Fig. 2, the HUVECs were observed to be single and round-shaped with podia. At $t = 24$ h,

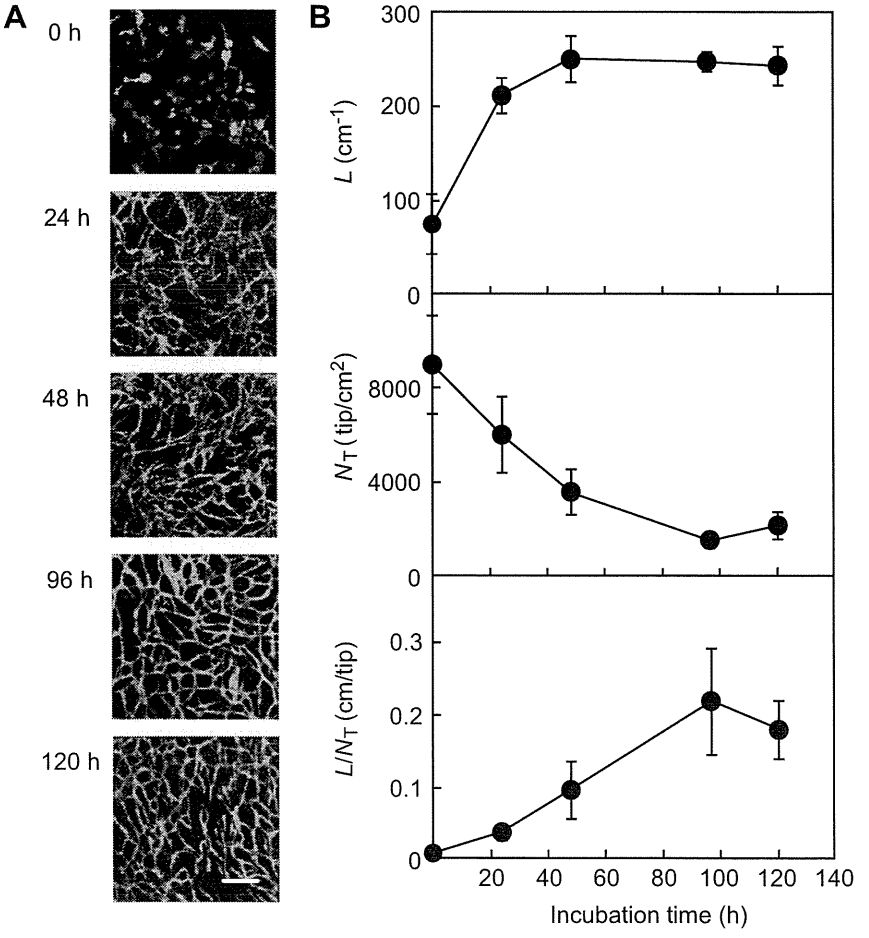

Fig. 2. Time course of HUVEC network formation inside the five-layered HSMM sheet at an initial HUVEC density (X_0) of 1.29 × 10^4 cells/cm^2. A: Horizontal images of HUVEC morphology. Scale bar: 200 μm. B: Evaluation of HUVEC network formation with image processing. L: total length (cm^{-1}), N_T: total tip number (tip/cm^2), L/N_T: extent of network formation (cm/tip). The bars show the standard deviation (SD) ($n = 3$).

most of the HUVECs were found to have elongated for initiation of migration in the sheet, resulting in an increase in L. With further prolongation of the incubation period beyond $t = 48$ h, the level of L was constant, i.e., the HUVECs did not grow further. In addition, the HUVECs began to encounter and connect with each other, resulting in a decrease in N_T until $t = 96$ h. Smooth connections of the HUVECs appeared at $t = 96$ h, which suggested the maturation of the HUVEC network. These behaviors were reflected by an increase in L/N_T although a slight decay of the connections occurred at $t = 120$ h. The maximum value of L/N_T was $= 0.22 \pm 0.07$ cm/tip at $t = 96$ h, which was 5.6 times higher than the value at $t = 24$ h.

3.2. Vertical migration of HUVECs during network formation

During network formation, the HUVECs were initially localized at the bottom of the HSMM sheet and then vertically migrated into the inner portion of the sheet to form aggregates with a lumen structure inside the sheet (Supplementary Fig. 2). To estimate the vertical migration of the HUVECs, their spatial distribution pattern was obtained as shown in Fig. 3. At the beginning ($t = 0$), the frequency of green cells (HUVECs) f_G was the highest in the first layer from the bottom surface, i.e., most of HUVECs were located at the bottom of the HSMM sheet. A broader distribution of f_G was obtained at $t = 24$ h, meaning the HUVEC migration toward the upper layers of sheet. In addition, the migration of the HUVECs was much faster than that of HSMMs because of the broader distribution of the HUVECs at $t = 24$ h (Supplementary Fig. 3). At $t = 96$ h, HUVECs inhabited the middle layer, with $f_G = 0.40$ and 0.30 in the second and third layers, respectively, which were higher than the values in the corresponding bottom and top layers. Fig. 3B and Supplementary movie 1 depict the aggregate shape of the HUVECs in the sheet at $t = 96$ h. The HUVECs in the middle layer formed a net-shaped aggregate to generate the network, whereas those in the top layer formed an island-shaped aggregate, which indicates that the shape of the HUVEC aggregate depended on their location in the sheet.

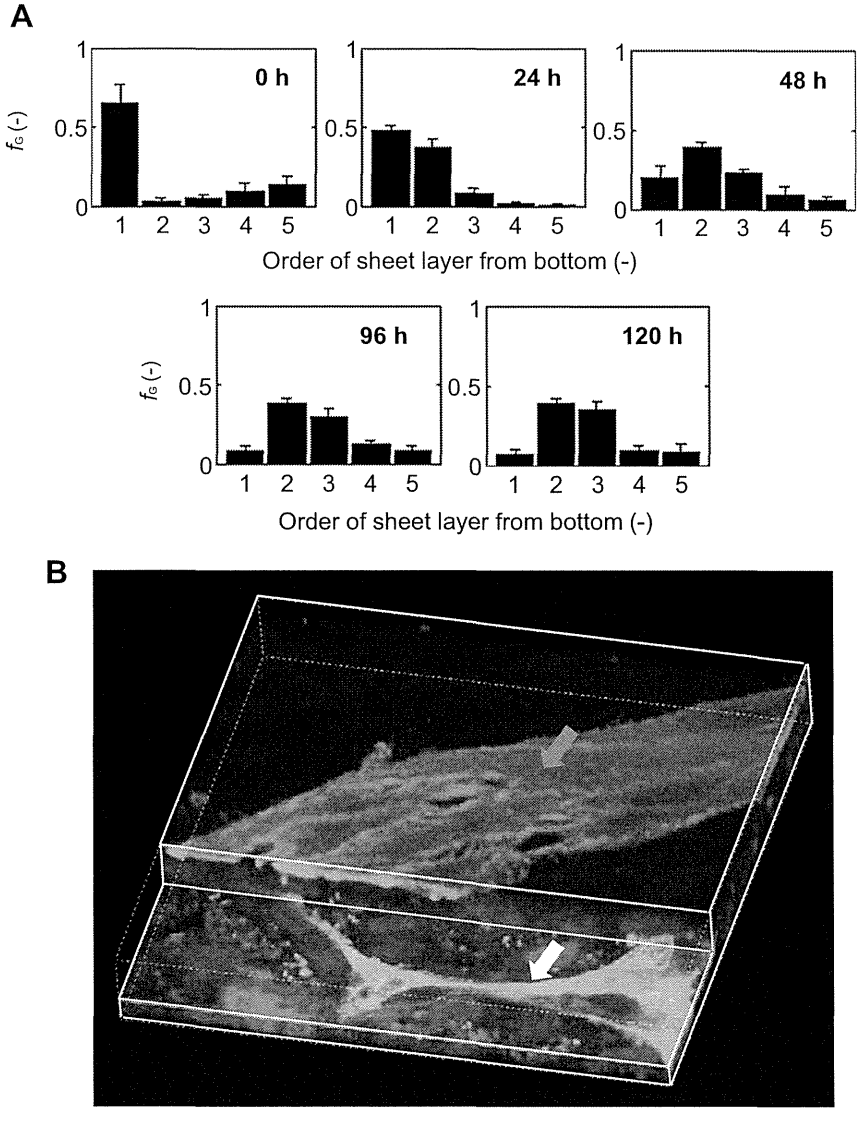

Fig. 3. Vertical analysis of HUVEC network formation inside the five-layered HSMM sheet at an initial HUVEC density (X_0) of 1.29×10^4 cells/cm^2. A: Time course of the spatial distribution of HUVECs (f_G) in each layer of the HSMM sheet. Bars show the standard deviation (SD) ($n = 3$). B: Three-dimensional image of HSMM sheet showing different shapes of HUVEC aggregates at different positions in/on the sheet at $t = 96$ h. The white arrow indicates net-shaped aggregation (network) in the middle layer of the cell sheet. The red arrow indicates island-shaped aggregation in the top layer on the cell sheet. (For interpretation of the references to colour in this figure legend, the reader is referred to the web version of this article.)